

# The Formation of the First Massive Black Holes

Zoltán Haiman

**Abstract** Supermassive black holes (SMBHs) are common in local galactic nuclei, and SMBHs as massive as several billion solar masses already exist at redshift  $z = 6$ . These earliest SMBHs may grow by the combination of radiation–pressure–limited accretion and mergers of stellar-mass seed BHs, left behind by the first generation of metal-free stars, or may be formed by more rapid direct collapse of gas in rare special environments where dense gas can accumulate without first fragmenting into stars. This chapter offers a review of these two competing scenarios, as well as some more exotic alternative ideas. It also briefly discusses how the different models may be distinguished in the future by observations with *JWST*, *LISA* and other instruments.

## 1 Introduction

The discovery of about two dozen bright quasars with luminosities  $\gtrsim 10^{47}$  erg s $^{-1}$  at redshift  $z \simeq 6$  suggests that some supermassive black (SMBHs) as massive as a few  $\times 10^9 M_{\odot}$  have been already assembled when the universe was less than 1 Gyr old (see, e.g., ref. [61] for a review). These high-redshift quasars are exceedingly rare, with a space density of order  $\sim 1 \text{Gpc}^{-3}$ , and can only be found in large surveys of the sky, such as the Sloan Digital Sky Survey (SDSS), or the smaller–area but deeper CFHQS [284] and UKIDSS [146] surveys. These quasars overall appear to be “fully developed”, with spectra and metallicity patterns that appear remarkably similar to their counterparts at moderate redshifts [62]. Indeed, if one selects individual quasars with the same luminosity, their properties show little evolution with cosmic epoch.<sup>1</sup> This implies that the behavior of individual quasars is proba-

---

Zoltán Haiman

Department of Astronomy, Columbia University, 550 West 120th Street, New York, NY 10027  
e-mail: zoltan@astro.columbia.edu

<sup>1</sup> A few possibly important exceptions to this are discussed in § 4.1.

bly determined by local physics near the SMBH and is not directly coupled to the cosmological context in which the SMBH is embedded. However, it is clear that the quasar population as a whole does evolve over cosmic timescales. Observations from  $0 \lesssim z \lesssim 6$  in the optical (e.g., the Anglo-Australian Telescope’s Two Degree Field, or 2dF, and the Sloan Digital Sky Survey, or SDSS) and radio bands [228] show a pronounced peak in the abundance of bright quasars at  $z \approx 2.5$ . A similar behavior has been confirmed in X-ray observations [238].

The cosmic evolution of quasar black holes between  $0 \lesssim z \lesssim 6$  is likely driven by a mechanism other than local physics near the hole. This is reinforced by the fact that the timescale of activity of individual quasars is significantly shorter than cosmic timescales at  $z \lesssim 6$ , both on theoretical grounds ( $\sim 4 \times 10^7$  yr, the e-folding time for the growth of mass in a SMBH, whose accretion converts mass to radiation with an efficiency of  $\varepsilon = \dot{M}c^2/L_{\text{Edd}} \sim 10\%$ ) and is limited by its own [Eddington] luminosity), and using the duty cycle of quasar activity inferred from various observations (also  $\sim 10^7$  yr but with large uncertainties, e.g. [160] and references therein; see also [91, 218, 221, 222]).

In the cosmological context, it is tempting to link the evolution of massive quasar black holes with that of dark matter (DM) halos condensing in a Cold Dark Matter (CDM) dominated universe, as the halo population naturally evolves on cosmic timescales [57]. Indeed, this connection has proven enormously fruitful and has resulted in the following broad picture: the first massive astrophysical black holes appear at high redshifts ( $z \gtrsim 10$ ) in the shallow potential wells of low mass ( $\lesssim 10^8 M_\odot$ ) dark matter halos. These black holes grow by mergers and gas accretion, evolve into the population of bright quasars observed at lower redshifts, and eventually leave the SMBH remnants that are ubiquitous at the centers of galaxies in the nearby universe.

In this picture, the presence of  $\text{few} \times 10^9 M_\odot$  SMBHs at  $z > 6$  presents a puzzle [99]<sup>2</sup>. Metal-free stars, with masses  $\sim 100 M_\odot$ , are expected to form at redshifts as high as  $z \gtrsim 25$  [3, 35, 299], and leave behind remnant BHs with similar masses [38, 106]. However, the natural time-scale, i.e. the Eddington time, for growing these seed BHs by  $\gtrsim 7$  orders of magnitude in mass is comparable to the age of the universe (e.g. ref. [99]). This makes it difficult to reach  $10^9 M_\odot$  without a phase of rapid (at least modestly super-Eddington) accretion, unless a list of optimistic assumptions are made in hierarchical merger models, in which multiple seed BHs are allowed to grow without interruption, and to combine into a single SMBH [86, 296, 33, 226, 276, 191, 150, 235, 250].

An alternative class of explanations involves yet more rapid gas accretion or collapse [182, 37, 138, 152, 240, 25, 273, 287, 203, 210, 217]. In this family of models, primordial gas collapses rapidly into a SMBH as massive as  $10^4 - 10^6 M_\odot$ , either directly, or possibly by accreting onto a pre-existing smaller seed BH [275], or going through the intermediate state of a very massive star [37], a “quasistar” [23], or a dense stellar cluster [186, 49]. These so-called “direct collapse” models involve metal-free gas in relatively massive ( $\gtrsim 10^8 M_\odot$ ) dark matter halos at redshift  $z \gtrsim 10$ ,

---

<sup>2</sup> More generally, the non-trivial cosmological implications of the existence of massive BHs at early times was noted already when quasars were first found at redshifts  $z > 4$  [259].

with virial temperatures  $T_{\text{vir}} \gtrsim 10^4 \text{K}$ . The gas that cools and collapses in these halos must avoid fragmentation, shed angular momentum efficiently, and collapse rapidly.

Many uncertainties about each of the above scenarios remain, and the astrophysical process(es) responsible for the formation of the earliest massive black holes (and indeed for the presence of SMBHs at all redshifts) remain poorly understood. In this review, we focus on the emergence of the first generation of black holes, though many of the important questions are quite general and apply equally to subsequent generations of black holes. This review is organized as follows. In § 2, we describe theoretical expectations for the formation and growth of these black holes within the paradigm of hierarchical CDM cosmologies. In § 3, we “zoom in” and consider the local physics of black hole formation, and various pathways which could lead to the early presence of supermassive black holes. In § 4, we summarize several relevant recent observations that have implications for early black holes, and speculate on the power of future observations to probe the physics of the first BHs. We offer our conclusions in § 5.

This chapter is an expanded and updated version of an earlier review [100]. Another recent, complimentary review on SMBH formation at high redshift can be found in [271].

## 2 First Structure Formation

In this section, we sketch some basic theoretical arguments relevant to the formation of structure in the early universe. We then discuss formation mechanisms for SMBHs.

### 2.1 *Cosmological Perturbations as the Sites of the First Black Holes*

Measurements of the Cosmic Microwave Background (CMB) anisotropies by the *Wilkinson Microwave Anisotropy Probe (WMAP)*, determinations of the luminosity distance to distant type Ia Supernovae, and other observations have led to the emergence of a robust “best fit” cosmological model with energy densities in CDM and “dark energy” of  $(\Omega_{\text{M}}, \Omega_{\Lambda}) \approx (0.3, 0.7)$  (see, e.g. [137], for the seven-year *WMAP* results, and its combination with other datasets).

The growth of density fluctuations and their evolution into nonlinear dark matter structures can be followed in this cosmological model from first principles by semi-analytic methods [193, 230]. More recently, it has become possible to derive accurate dark matter halo mass functions directly in large cosmological N-body simulations [118], with different codes agreeing at the 10% level, and mass functions measured down masses as low as  $\sim 10^6 M_{\odot}$  and high redshifts as high as  $z \approx 30$  (e.g. [153, 200]).

Within the  $\Lambda$ CDM model, with a scale-invariant primordial power spectrum, robust predictions can therefore be made for the dark matter halos. Structure formation in such a universe is “bottom-up”, with low-mass halos condensing first. Halos with the masses of globular clusters ( $10^{5-6} M_{\odot}$ ) are predicted to have condensed from  $\sim 3\sigma$  peaks of the initial primordial density field as early as  $\sim 1\%$  of the current age of the universe, or at redshifts of  $z \sim 25$ . These predictions are limited mainly by the 5 – 10% uncertainty in the normalization of the primordial power spectrum,  $\sigma_8$ , and by the need to extrapolate the power-spectrum 2-3 orders of magnitude below the scales on which it has been directly constrained. In warm dark matter models, with particle masses of order  $\sim 1\text{keV}$  or less, free-streaming would result in a sharp exponential suppression of the fluctuation power on the relevant scales (masses below  $10^8 M_{\odot}$ ), and could significantly reduce the number of DM halos at the earliest redshifts [13, 300].

It is natural to identify the first collapsed DM halos as the sites where the first astrophysical objects, including the first black holes, were born. The nature of the objects that form in these early dark matter halos is currently one of the most rapidly evolving research frontiers in astronomy.

## 2.2 Chemistry and Gas Cooling at High Redshifts

Baryonic gas that falls into the earliest nonlinear dark matter halos is unable to cool efficiently, and is shock heated to the characteristic virial temperatures less than a few hundred Kelvin. It has long been pointed out [26, 202, 282] that such gas needs to lose its thermal energy efficiently (within about a dynamical time) in order to continue contracting, or in order to fragment. In the absence of any dissipation, it would simply reach hydrostatic equilibrium and would eventually be incorporated into a more massive halo further down the halo merger hierarchy. While the formation of nonlinear dark matter halos can be followed from first principles, the cooling and contraction of the baryons, and the ultimate formation of stars or black holes in these halos, is much more difficult to model *ab initio*.

The gas content of a cosmological perturbation can contract together with the dark matter only in dark halos above the cosmological Jeans mass,  $M_J \approx 10^4 M_{\odot} [(1+z)/11]^{3/2}$ , in which the gravity of dark matter can overwhelm thermal gas pressure. Recent work [256] has shown that immediately following recombination (at redshift  $z \sim 1,000$ ), the baryons develop coherent streaming motions relative to the dark matter, with relative speeds of order  $30 \text{ km s}^{-1}$ , on scales of a few Mpc. These relative velocities decay as  $\propto (1+z)$ , and reduce to  $\sim 1 \text{ km s}^{-1}$  by  $z \sim 30$ , comparable to the velocity dispersions in the smallest dark matter halos at this epoch. In the somewhat more massive halos in which the baryons can typically cool efficiently (with velocity dispersions of several  $\text{km s}^{-1}$  at  $z \lesssim 30$ ; see below), the streaming motions are expected to have at most a modest effect, reducing the gas fraction within the virial radius by a factor of  $\sim$ two [255, 159, 244, 78, 48]. However, as we will see below, the “stellar-seed” model for SMBH growth relies on one (or a few) “special”

rare seed BHs that form in  $\text{few} \times \sim 10^5 M_\odot$  halos at redshifts as high as  $z \sim 30$ . This scenario appears vulnerable to the streaming motions.

In the earliest, chemically pristine clouds, radiative cooling is dominated by  $\text{H}_2$  molecules. As a result, gas phase  $\text{H}_2$  “astro-chemistry” is likely to determine the epoch when the first stars and black holes appear (primordial molecular chemistry, focusing on the role of  $\text{H}_2$  early structure formation was reviewed by [4]). Several papers have constructed complete gas-phase reaction networks and identified the two possible ways of gas-phase formation of  $\text{H}_2$  via the  $\text{H}^-$  or  $\text{H}_2^+$  channels. These were applied to derive the  $\text{H}_2$  abundance under densities and temperatures expected in collapsing high redshift objects [108, 162, 190, 148, 224, 126, 125, 223]. Studies that incorporate  $\text{H}_2$  chemistry into cosmological models and that address issues such as non-equilibrium chemistry, dynamics, or radiative transfer have appeared relatively more recently. Ref [103] used spherically symmetric simulations to study the masses and redshifts of the earliest objects that can collapse and cool via  $\text{H}_2$ ; their findings were confirmed by a semi-analytic treatment [253]. The first fully three dimensional cosmological simulations that incorporate  $\text{H}_2$  chemistry and cooling date back to refs [189, 73] and [1].

The basic picture that emerged from these papers is as follows. The  $\text{H}_2$  fraction after recombination in the smooth “protogalactic” gas is small ( $x_{\text{H}_2} = n_{\text{H}_2}/n_{\text{H}} \sim 10^{-6}$ ). At high redshifts ( $z \gtrsim 100$ ),  $\text{H}_2$  formation is inhibited, even in overdense regions, because the required intermediaries  $\text{H}_2^+$  and  $\text{H}^-$  are dissociated by cosmic “microwave” background (CMB, but with the typical wavelength then in the infrared) photons. However, at lower redshifts, when the CMB photons redshift to lower energies, the intermediaries survive, and a sufficiently large  $\text{H}_2$  abundance builds up inside collapsed clouds ( $x_{\text{H}_2} \sim 10^{-3}$ ) at redshifts  $z \lesssim 100$  to cause cooling on a timescale shorter than the dynamical time. Sufficient  $\text{H}_2$  formation and cooling is, however, possible only if the gas reaches temperatures in excess of  $\sim 200$  K or masses of a few  $\times 10^5 M_\odot [(1+z)/11]^{-3/2}$  (note that while the cosmological Jeans mass increases with redshift, the mass corresponding to the cooling threshold, which is well approximated by a fixed virial temperature, has the opposite behavior and decreases at high redshift). The efficient gas cooling in these halos suggests that the first nonlinear objects in the universe were born inside  $\sim 10^5 M_\odot$  dark matter halos at redshifts of  $z \sim 20 - 30$ , corresponding to an  $\sim 3 - 4\sigma$  peaks of the primordial density peak (of course, yet rarer low-mass halos exist even earlier - the first one within our Hubble volume collapsing as early as  $z \approx 60$  [176]).

The behavior of metal-free gas in such a cosmological “minihalo” is a well posed problem that has been addressed in three dimensional numerical simulations. The first series of such simulations [2, 3, 34, 35, 298] were able to follow the contraction of gas to much higher densities than preceding studies. They have shown convergence toward a temperature/density regime of  $T \sim 200$  K,  $n \sim 10^4 \text{ cm}^{-3}$ , dictated by the critical density at which the excited states of  $\text{H}_2$  reach equilibrium and cooling becomes less efficient [67]. These simulations suggested that the gas does not fragment further into clumps below sizes of  $10^2 - 10^3 M_\odot$ , but rather it forms unusually massive stars. Very recent simulations reached higher resolution than the earlier ones, and, in some cases, using sink particles, were able to continue their runs be-

yond the point at which the first ultra-dense clump develops [258, 246, 77, 195]. These simulations suggest that at least in some cases, the gas in the central regions does, eventually, fragment into two or more distinct clumps, raising the possibility that the first stars formed in pairs, or even in higher-multiple systems.

The masses of the first stars would then presumably be reduced. The initial mass function (IMF) of the first stars is crucial, and is indeed one of the most important uncertainties for early BH formation. This is because massive stars would naturally leave behind black hole seeds, which can subsequently grow by mergers and accretion into the SMBHs. Interestingly, massive stars appear to have an “either/or” behavior. Non-rotating stars with masses between  $\sim 40 - 140 M_{\odot}$  and above  $\sim 260 M_{\odot}$  collapse directly into a black hole without an explosion, and hence without ejecting their metal yields into the surrounding medium, whereas stars in the range  $\sim 140 - 260 M_{\odot}$  explode as pair-instability supernovae without leaving a remnant [106]. In contrast, stars with initial masses  $\sim 25 - 40 M_{\odot}$  still leave BH remnants but also eject metals, whereas those with masses  $M \lesssim 25 M_{\odot}$  do not leave any BH remnants. This dichotomy is especially interesting because early massive stars are attractive candidates for polluting the IGM with metals at high redshifts [155, 281]. It is likely that the first stars had a range of masses, in which case they could contribute to both metal enrichment and to the seed black hole population, with a relative fraction that depends sensitively on their initial mass function (IMF).

### 3 Massive Black Hole Formation

Having reviewed the general problem of structure formation at high redshifts, we now focus on the question of how the first SMBHs were assembled. It is worth emphasizing that this is an unsolved problem – indeed, it is not entirely clear even whether the first nonlinear objects in the universe were stars or black holes, and whether galaxies or their central black holes formed first [87]. The leading ideas related to the formation of SMBHs at high redshifts can be broadly divided into three areas: (1) formation of seed black holes from “normal” stellar evolution and subsequent Eddington-limited accretion, (2) rapid direct collapse of gas to a SMBH, usually via a supermassive star/disk, and (3) formation of a SMBH (or an IMBH seed) by stellar dynamical processes in dense stellar systems, such as star clusters or galactic nuclei. It is, of course, possible that all of these processes could be relevant [22, 201].

### 3.1 Growth from Stellar-Mass Seeds

#### 3.1.1 Basic Ingredients and Uncertainties

Perhaps the most natural possibility is that early SMBHs grow by gas accretion out of stellar-mass seed black holes, left behind by early generation of massive stars. If the subsequent gas accretion obeys the Eddington limit and the hole shines with a radiative efficiency of 10%, then the time it takes for a SMBH to grow to the size of  $3 \times 10^9 M_\odot$  from a stellar seed of  $\sim 100 M_\odot$  is  $3 \times 10^7 \ln(3 \times 10^9/100) \text{ yr} \sim 7 \times 10^8 \text{ yr}$ . This is comparable to the age of the universe at  $z = 6$  ( $\sim 9 \times 10^8 \text{ yr}$  for a flat  $\Lambda$ CDM universe with  $H_0 = 70 \text{ km s}^{-1} \text{ Mpc}^{-1}$  and  $\Omega_M = 0.3$ ). Therefore, the presence of these SMBHs is consistent with the simplest model for black hole growth, provided that (i) *the seeds are present early on (at  $z \gtrsim 15$ ; see below)*, (ii) *and the near-Eddington growth is uninterrupted*. As the  $\sim 10^{5-6} M_\odot$  host halo of the initial seed BH gets incorporated into the  $\sim 10^{12-13} M_\odot$  host halo of the  $z \approx 6$  SMBH, it grows by  $\sim 7$  orders in magnitude, and experiences a large number of mergers with other, comparable-sized, halos. These merger partners may (or may not) have a growing BH at their centers. Therefore, these mergers need to be taken into account, and the “stellar seed” model most likely can not be viewed as that of a single seed BH, growing in isolation.

Several authors have worked out the growth of SMBHs from stellar-mass seeds, by following the build-up of dark DM halos, and using simple prescriptions to track the formation of seed BHs, their subsequent growth by accretion, and their mergers. This can be done either semi-analytically [99, 295, 86, 226], using Monte-Carlo realizations of the DM merger trees [296, 33, 276, 250], or based on cosmological hydrodynamics simulations [150, 191, 235]. As noted in the Introduction, the uncertainties about the statistics of the DM halo merger trees are essentially negligible<sup>3</sup>, since DM halo formation has been directly resolved in numerical simulations at the relevant low masses (down to  $\sim 10^6 M_\odot$ ) and high redshifts (out to  $z \approx 30$ ). The most important – and still highly uncertain – ingredients of this ‘stellar seed’ scenario can be summarized as follows.

(i) *What is the smallest possible mass (or virial temperature,  $T_{\text{seed}}$ ) for early DM halos in which PopIII stars can form?* A reasonable answer is  $T_{\text{seed}} = \text{few} \times 100 \text{ K}$ , which allows molecular  $\text{H}_2$ -cooling [103, 253].

(ii) *In what fraction ( $f_{\text{seed}}$ ) of these halos do seed BHs actually form?* This is a much more difficult question, since various feedback processes (due to radiation, metal pollution, or mechanical energy deposition) could suppress PopIII star formation in the vast majority of early low-mass halos ([88, 92]; see also a recent review [36]). Interestingly, the *WMAP* measurement of the electron scattering optical depth provides empirical evidence that such negative feedback took place early on and shaped the reionization history [89]. The answer also depends on the IMF of

<sup>3</sup> At least in principle, since halo mass functions in large N-body simulations agree at the few percent level. In practice, however, there can be significant disagreements between Monte-Carlo halo merger trees made with different algorithms [305].



PopIII stars, since, as noted above, whether the stars leave a BH remnant or explode as pair instability SNe depends on their masses. The dividing mass,  $\approx 25 M_{\odot}$ , was evaluated in non-rotating stellar evolution models [106], whereas recent simulations indicate that the first stars in minihalos have significant rotation [245]. Rotation can help drive winds and prevent BH formation entirely, or can produce a hypernova and reduce the mass of the remnant BH. Finally the velocity dispersions of the lowest-mass minihalos are only a few  $\text{km s}^{-1}$ , only a factor of few higher than the residual bulk streaming motions between the gas and the DM halo at  $z \gtrsim 20$ . These streaming motions can therefore reduce the gas fractions in the earliest minihalos and also lower the stellar masses by driving turbulence [78].

(iii) *What is the time-averaged accretion rate of the seed BHs?* This is conveniently parameterized by a duty cycle  $f_{\text{duty}}$ , defined as the fraction of the mass accretion rate that would produce the Eddington luminosity, if  $\epsilon \approx 10\%$  of the rest mass was converted to radiation (so that  $f_{\text{duty}} = 1$  is the fiducial Eddington rate). Radiative feedback is usually expected to lead to sub-Eddington rates (e.g. [6]), and in spherical symmetry, the accretion was recently shown to be episodic, with  $f_{\text{duty}} \approx 0.3$  [173]. The expectation is therefore that  $f_{\text{duty}}$  is less than unity. In practice, if the accretion is radiatively inefficient, or if the radiation is trapped or is beamed and “leaks out”, then  $f_{\text{duty}}$  could exceed unity (see more on this below).

(iv) *Finally, what happens when DM halos merge?* The simplest and most optimistic assumption is that the BHs promptly coalesce, as well. However, even if dynamical friction on the DM (and on any stars present in later stages of the merger hierarchy) is efficient, it is possible that, due to the radiation of its parent star, the remnant BHs are no longer embedded in dense enough gas to allow this. Furthermore, even if the BHs coalesce, the merged binary BH can suffer strong gravitational recoil at the time of the merger, due to the linear momentum carried by the anisotropic emission of gravitational waves (e.g. [11] and references therein). Such a “kick” can eject the BH from the shallow potential wells ( $\sim 1\text{km/s}$ ) of the early halos, and the BH will be effectively lost. While kicks for comparable-mass BHs with random spins are of the order of  $\sim 100\text{ km/s}$ , the kick speed depends strongly on the mass ratio and on the spin vectors of the two BHs. In particular, kicks become very small ( $\lesssim 1\text{km/s}$ ) for mass ratios  $q \equiv M_1/M_2 \lesssim 10^{-2}$ , irrespective of BH spins (e.g. [11]). This may be key to avoid losing growing seed BHs by ejection, and thus for the buildup of SMBHs early on.

### 3.1.2 Worked Illustrative Examples

In Figure 1, we show SMBH mass functions at  $z = 6$ , illustrating the impact of three of the most uncertain basic assumptions above, taken from a recent example of the Monte Carlo merger tree approach [250]. The mass functions were constructed from the merger histories of  $\approx 10^5$  DM halos with masses  $M > 10^8 M_{\odot}$  at redshift  $z = 6$ . The upper right region in each panel, demarcated by the red dashed rectangle, shows the observational constraint on the SMBH space density. Each galaxy was modeled with a spherically symmetric mass distribution consisting of a DM halo



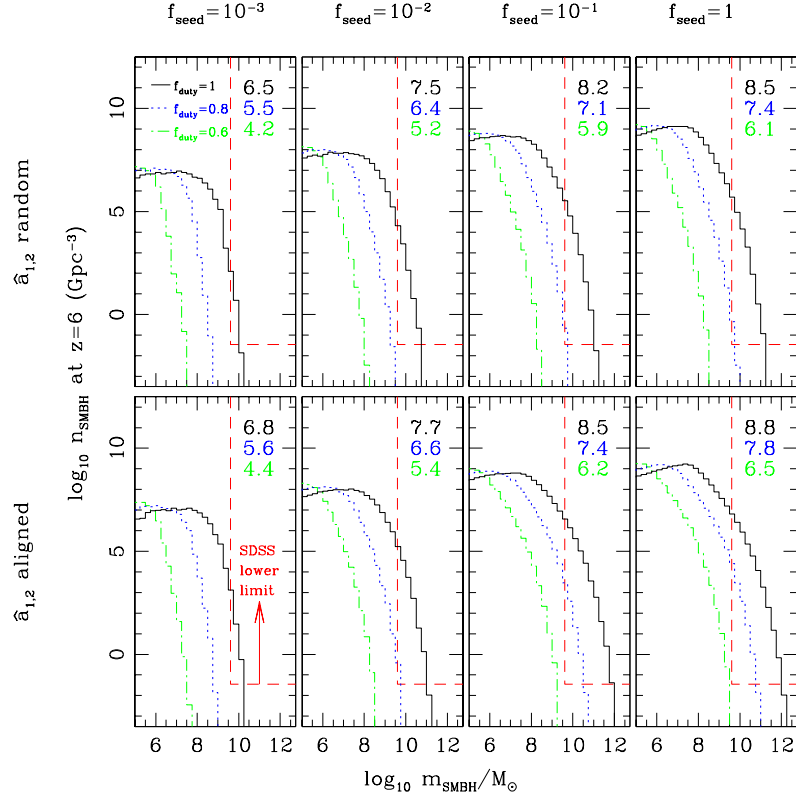


**Fig. 1** The comoving number densities of SMBHs in different mass bins at redshift  $z = 6$ . The 24 different models shown in the figure assume different parameter combinations as follows. The columns, from left to right, adopt  $f_{\text{seed}} = 10^{-3}$ ,  $10^{-2}$ ,  $10^{-1}$ , 1. The top row assumes a random binary spin orientation, and the bottom row assumes that BH spins are aligned with the binary’s orbital angular momentum. In each panel, the time-averaged mass-accretion rates, in Eddington units, are assumed to be either  $f_{\text{duty}} = 1$  (black solid curves),  $f_{\text{duty}} = 0.8$  (blue dotted), and  $f_{\text{duty}} = 0.6$  (green dash-dotted). The numbers in the upper-right corners represent the total mass density in SMBHs  $\log_{10}[\rho_{\bullet}/(M_{\odot} \text{Mpc}^{-3})]$  for each model. The red dashed line demarcates the abundance of  $z \approx 6$  SMBHs with  $m \gtrsim 10^{9.6} M_{\odot}$  already observed in the SDSS (adapted from ref. [250]).

with a Navarro-Frenk-White (NFW) profile [177], and a more cuspy baryonic component (with  $\rho \propto r^{-2.2}$ , suggested by 3D simulations). At the time of a merger, the trajectories of kicked BH – ejections, or oscillations damped by dynamical friction – were followed explicitly by one-dimensional orbital calculations.

Figure 1 shows that a robust conclusion for a model to produce enough  $z = 6$  SMBHs is that  $f_{\text{duty}} \gtrsim 0.6$  – namely the  $\approx 100 M_{\odot}$  stellar seed BHs must accrete near the Eddington rate nearly all the time. (Note that this value is excluded in the spherically symmetric case [174].) The initial BH occupation fraction also has

to be  $f_{\text{seed}} \gtrsim 10^{-3}$ . Another interesting, and less intuitive conclusion, is that if the initial seeds are rare ( $f_{\text{seed}} = 10^{-3} - 10^{-2}$ ), then gravitational kicks do *not* have a big impact, and it makes little difference to the SMBH mass function whether spins are aligned or randomly oriented (this can be seen by comparing the bottom and top panels in Fig. 1). This is because the few “lucky” seeds that form earliest (at  $z \gtrsim 25$ ) have a chance to grow by  $\gtrsim$  two orders of magnitude in mass before encountering their first merger. The masses of the two BHs at this first merger are then very unequal ( $q = M_1/M_2 \lesssim 0.01$ ), making kick velocities too low to lead to ejection. It is important to emphasize, however, that the model trajectories for the kicked BHs assume spherical symmetry [156, 31, 80, 250]. In gas-rich galaxies, most of the dynamical friction occurs due to the dense baryons at the center of the potential [250, 82]. In asymmetric potentials, the kicked BH does not return to the central region - its oscillations are damped less quickly [81] and the accretion rate onto the oscillating hole is also suppressed.

An important additional issue is that in those models that satisfy the observational constraint on the SMBH abundance, the massive end of the SMBH mass function is extremely steep. This prediction is not surprising, as the most massive SMBHs reside in few  $\times 10^{12} M_{\odot}$  halos, which probe the  $5\sigma$  tail of the halo mass function at  $z = 6$  (and there are indeed  $\approx 10^8$  (!) times as many few  $\times 10^9 M_{\odot}$  halos, which host  $\sim 10^6 M_{\odot}$  BHs). As a result, the total mass density in SMBHs with masses above  $\gtrsim 10^5 M_{\odot}$  BHs (shown by the numbers in the upper right corners in Figure 1) are overpredicted by a factor of  $10^2 - 10^3$ . Note that these numbers indicate the mass in SMBHs that avoided ejection due to kicks, and remained in galactic centers (in some of the models, a significant fraction of the BHs are ejected and form intergalactic BHs; there is no obvious means to detect these [250]). The mass density of such nuclear SMBHs at  $z \approx 0$  can be inferred from the observed correlations between BH masses and host galaxy properties (such as the masses or velocity dispersions of the host halos; e.g. [64]). The result is several  $\times 10^5 M_{\odot} \text{Mpc}^{-3}$ ; furthermore, the expectation is that most ( $\gtrsim 90\%$ ) of this mass was accreted well after  $z = 6$  [218]. Some strong feedback is therefore needed to eliminate this significant overprediction. Possible candidates for this are radiative feedback internal to halos, which maintains the “ $M - \sigma$  relation” in ultra-high redshift, low-mass halos, or the termination of PopIII star formation, at redshifts as high as  $z \sim 20$ , due to Lyman Werner radiation [89] or metal pollution [36].

Finally, it is worth emphasizing that the mass accretion rate corresponding to the Eddington limit – for the fiducial radiative efficiency of  $\epsilon \equiv L/\dot{m}c^2 = 0.1$  for converting mass to radiation – would need to be exceeded only by a factor of a  $\sim$ few to make the growth from stellar seeds much easier. Modestly exceeding the Eddington rate is theoretically certainly plausible (see below): density inhomogeneities can allow radiation to leak out of low density regions while most of the accreting matter can be contained in high density regions. For example, magnetized radiation dominated accretion disks are subject to a “photon bubble” instability that nonlinearly appears to lead to strong density inhomogeneities (e.g. [18]). Nevertheless, observations have so far not revealed systems that sustain super-Eddington accretion for

extended periods; it would then still have to be explained why the  $z \approx 6$  quasar BHs have this uniquely different behaviour.

### 3.1.3 Accretion versus Mergers

Mergers between halos can help build up the mass of individual black holes (without significantly changing the total mass of the population), provided that the central black holes in the halos coalesce rapidly. The mean accretion efficiency of  $\sim 10\%$  inferred from comparing the local black hole mass density with the integrated quasar light suggests that accretion dominates at least the last e-folding of the black hole mass [302, 218]. Mergers may, however, be significant earlier on [91]. In addition, uncertainties in the *expected* radiative efficiency of black hole accretion limit how accurately one can constrain the growth of black hole mass by mergers. For example, if the typical efficiency was  $\approx 40\%$ , as for a maximally rotating Kerr black hole, then the Eddington-limited mass accretion rate would be decreased correspondingly, and mergers could dominate black hole growth (on the other hand, note that multiple mergers would have a tendency to cancel the black hole spin; [112]). In order for mergers to contribute significantly to the growth of individual black hole masses, stellar seeds must be present in large numbers, in the most of the numerous mini-halos that form at  $z \gtrsim 15$ , down to small halo masses.

The balance between growth through BH mergers and growth through gas accretion is indeed a key characteristic of any SMBH assembly scenario. For concreteness, consider possible merger histories for the  $z = 5.82$  SDSS quasar SDSS 1044-0125 ([99], the following arguments would be stronger for more luminous quasars at higher redshift). One can estimate the mass of the dark matter halo harboring the quasar by its abundance. SDSS searched a comoving volume of  $\sim 1 \text{ Gpc}^3$  to find each quasar. Assuming a duty cycle of a few times  $10^7$  years, one estimates that the dark matter halos corresponding to this space density have masses of  $10^{13} M_\odot$  (using the halo mass function in ref. [118], the original Press-Schechter formula [193] would give a similar answer). A  $10^{13} M_\odot$  halo at  $z = 6$  typically has only  $\sim 10$  progenitors with circular velocities of  $v > 50 \text{ km s}^{-1}$  (the other progenitors being smaller). This implies that mergers can only help build up the black hole mass if seed black holes are present in progenitor halos with much smaller masses. A cutoff in the black hole mass function in halos with circular velocities below  $v = 50 \text{ km s}^{-1}$  would be justified if the cosmic ultraviolet background could suppress gas infall into smaller halos [56, 254, 178, 133]. However, one-dimensional gas collapse models with radiative feedback [52] have shown that this suppression is ineffective at redshifts beyond  $z \gtrsim 6$ . Thus, there is no obvious obstacle to forming seed black holes in halos down to  $v \sim 10 \text{ km s}^{-1}$  (below this threshold, atomic H cooling becomes inefficient, and  $\text{H}_2$ -photodissociation can be a limitation).

In the illustrative models discussed in the previous section, which successfully reproduce the abundance of the  $\times 10^9 M_\odot$  SDSS quasar BHs, gas accretion accounts for the vast majority of the growth (in the sense that if the seed BHs were simply added together without any further accretion, the resulting total BH mass at  $z = 6$

would be reduced by many orders of magnitude; see Table 3 in [250]). However, in versions of these models in which BH growth is assumed to be self-regulating, accretion is much less important. Such models essentially describe the most heavily merger-driven scenarios possible, requiring accretion-driven growth of as little as a factor of a few. This is not surprising: placing a seed black hole in each arbitrarily low mass progenitor halo, with the same black hole mass to halo mass ratio as inferred for the SDSS quasars ( $M_{\bullet}/M_{\text{halo}} \sim 10^{-4}$ ), could account for the observed black hole masses in quasars by  $z = 6$ , even without *any* gas accretion [91].

A further important unsolved question is whether halo mergers necessarily lead to black hole mergers at all (see, e.g., [168] for a review). During a galaxy merger, the black holes sink via dynamical friction to the center of the galaxy and form a tight black hole binary in the nucleus. In normal galaxies with a stellar component in the nucleus, the black hole binary can continue to shrink by ejecting low-angular momentum stars that pass close to the binary (those in the “loss cone”). This process, however, clearly does not operate in the earliest stages of structure formation, when there are at most a few stars (if any) present in the merging mini-galaxies. Even at the later states, this process is inefficient, at least in spherical stellar systems, because the loss cone must be replenished by two-body relaxation. The black hole binary thus appears to stall and cannot coalesce even during a Hubble time [20].

Several ideas for circumventing this difficulty have been proposed. At later stages, in triaxial stellar populations, low-angular momentum orbits are populated much more efficiently because the stellar orbits can be chaotic; the resulting binary decay times are in many cases significantly less than a Hubble time, even if only a few percent of the stellar mass is on chaotic orbits (e.g., [301, 169, 194, 158]). In the earliest galaxies without large stellar populations, the coalescence of BHs must be facilitated by gas physics. If circumbinary gas is present and forms a thin accretion disk, then BH-disk interactions can drag the binary together, in a manner similar to Type II migration in planetary systems. The main difference from the planet case is that at least for nearly equal mass binaries, the secondary BH’s mass will far exceed the mass of the disk, which slows down the migration (see [95] for a comprehensive discussion, and [76, 8, 60] for examples of earlier work). A binary BH embedded in a spherical gas cloud is also facilitated by gaseous torques [60]; this case is much less well explored, but is likely to be more relevant to the earliest stages of the growth in the stellar-seed models, in halos without stars and with potential wells too shallow to support a thin disk. Finally, if SMBHs are brought together by successive halo mergers at a rate higher than the rate at which they can coalesce, then one or more of the BHs can be ejected out of the nucleus of the merger remnant by the slingshot mechanism [209]. This could have implications for SMBH mass build-up in principle; in practice, more recent work on the dynamics of triple BHs indicate that ejections are relatively rare, and in the majority of cases, at least two of the BHs coalesce [110, 7].

### 3.1.4 Super-Eddington Mass Accretion

If mass is supplied to a black hole at  $\dot{m} \equiv \dot{M}/\dot{M}_{Edd} \gg 1$ , the photons are trapped in the inflowing gas because the photon diffusion time out of the flow becomes longer than the time it takes the gas to accrete into the black hole (e.g. [16, 21]). The resulting accretion is thus not via the usual thin disk [216], but rather via a radiatively inefficient flow (RIAF). The luminosity is still set by the Eddington limit, but most of the gravitational binding energy released by the accretion process is not radiated away (being trapped in the flow).

It is attractive to assume that the growth of SMBHs at high redshifts proceeds via such an optically thick, photon trapped accretion flow with  $\dot{m} \gg 1$ . Indeed, it would be a remarkable coincidence if the mass supply rate were precisely  $\sim \dot{M}_{Edd}$  (required for a thin accretion disk) during the entire growth of massive black holes. It is more likely that the mass supply rate is initially much larger in the dense environments of high redshift galaxies ( $\dot{m} \gg 1$ ) and then slowly decreases with time as the galaxy is assembled and the BH gains mass (e.g., [239, 40]).

Three-dimensional simulations for the cooling and collapse of gas into the first minihalos find that  $H_2$  cooling reduces gas temperatures to a few  $\times 100$ K and produces a quasi-static contraction, with relatively low mass accretion rates of  $10^{-3} - 10^{-2} M_\odot \text{ yr}^{-1}$  (e.g. [3]). This external mass-supply rate would still correspond to a super-Eddington growth rate for a BH with a mass of  $\lesssim 10^5 M_\odot$ . However, there is another limitation: within a Kelvin-Helmholtz time of  $\sim 10^5$  years, only a few  $\times 100 M_\odot$  of material is accreted to the center (this is shown explicitly in Figure 4). Much more mass than this is then unlikely to be incorporated onto the central proto-star, before it settles to the main sequence. Radiative feedback from the proto-star (in the form of  $H_2$  dissociation, Lyman  $\alpha$  radiation pressure, and ultimately, photoionization heating) on the infalling envelope was found to limit the final mass of the star to  $\approx 140 M_\odot$  [249, 165].

On the other hand, in more massive halos *provided that  $H_2$  cooling can be disabled throughout the entire time of the collapse*, the gas temperature is set by atomic H cooling and remains near  $10^4$ K. In a self-gravitating gas, the mass accretion rate is of order  $\sim c_s^3/G \propto T^{3/2}/G$  (e.g. [234]). Three-dimensional simulations have confirmed this scaling (e.g. [187, 217]), and in halos with  $T_{\text{vir}} \sim 10^4$ K, have found mass accretion rates of  $\sim 1 M_\odot \text{ yr}^{-1}$  [217]. As shown explicitly in Figure 4, with this higher mass accretion rate, the mass that can be accumulated in the nucleus within a Kelvin-Helmholtz time is increased to  $10^5 M_\odot$ .

Theoretical models for the accretion on much smaller spatial scales (not resolved in the above simulations) imply that even if  $\dot{m} \gg 1$ , only a small fraction of the mass supplied to the black hole actually reaches the horizon; most of it is driven away in an outflow (see, e.g., simulations of RIAFs [248, 247, 105, 114, 196]; and analytic models [29, 30, 197]). The accretion rate onto a black hole thus probably cannot exceed  $\sim \dot{M}_{Edd}$  by a very large factor, even if the mass supply rate from larger radii is large (see [216] for an early discussion of this point).

The above discussion focuses on whether highly super-Eddington accretion is possible. The question of whether the Eddington limit for the luminosity can be

exceeded by a modest factor of  $\sim 10$  is a bit more subtle. Magnetized radiation dominated accretion disks are subject to a “photon bubble” instability that nonlinearly appears to lead to strong density inhomogeneities (see, in particular, [9, 68, 17, 28, 18]). Density inhomogeneities allow super-Eddington fluxes from the accretion flow because radiation leaks out of the low density regions while most of the matter is contained in high density regions. Ref. [18] estimates that the Eddington limit can potentially be exceeded by a factor of  $\sim 10 - 100$ . This would allow much more rapid growth of black holes at high redshifts, circumventing the above arguments that seed black holes at  $z \sim 15$  are required. Magneto-hydrodynamic (MHD) simulations of radiation dominated accretion flows have confirmed the rapid growth of unstable short-wavelength modes, with the development of large density variations. Inhomogeneities then allow the radiation to diffuse outward five times more rapidly than in a disk in hydrostatic equilibrium with no magnetic fields [260]. Explicit models for such slim, porous, accretion disks have been constructed recently [54]. In these models, when the external mass accretion rate is  $10\text{--}20 \times \dot{M}_{Edd}$ , despite the presence of winds, a super-critical fraction,  $2.6\text{--}3.8 \dot{M}_{Edd}$ , was indeed found to reach the central SMBH.

### 3.2 Growth by Rapid Direct Collapse

An appealing alternative idea is to produce, say, a  $10^5 M_\odot$  SMBH “directly” – i.e. much faster than this would take under Eddington–limited accretion from a stellar seed. This would clearly be helpful to explain the high–redshift SMBHs. In this context, the crucial question is whether gas can accrete at a highly super-Eddington rate onto a black hole, i.e., with  $\dot{M} \gg \dot{M}_{Edd}$ , where  $\dot{M}_{Edd} = 10L_{Edd}/c^2 \approx 1.7M_8 M_\odot \text{ yr}^{-1}$  is the accretion rate that would produce an Eddington luminosity if accretion onto a black hole of mass  $10^8 M_8 M_\odot$  proceeded with 10% radiative efficiency. If so, this could lead to rapid black hole growth at high redshifts. Constraints on BH seeds and their formation redshifts would therefore be much less stringent.

#### 3.2.1 Rapid Collapse of Gas in $T_{\text{vir}} \gtrsim 10^4 \text{K}$ Halos

SMBHs may form directly by the collapse of gas clouds at high redshifts, likely via an intermediate stage of a supermassive star or disk. The gas must not only shed angular momentum efficiently and collapse rapidly, but must also then avoid fragmentation. Whether fragmentation of the gas cloud into stars can be avoided is particularly questionable, in view of the large angular momentum barrier that must be overcome to reach small scales in a galactic nucleus (forming an SMBH through a dense stellar cluster is another option, discussed in the next section).

The most promising locations for such rapid “direct collapse” are at the centers of halos with  $T_{\text{vir}} \sim 10^4 \text{K}$ . In the past several years, many authors have sketched how gas may collapse rapidly, without fragmentation, in these halos. The essential

idea is that when contracting gas in a protogalactic nucleus becomes optically thick and radiation pressure supported, it becomes less susceptible to fragmentation and star formation. It is, however, unlikely that radiation pressure becomes important before angular momentum does, implying that the gas forms a viscous accretion disk in the galactic nucleus (fragmentation before the disk forms can also be avoided if the forming fragments collide and “coalesce” before they can separate into discrete dense clumps [127]). On the other hand, if self-gravitating, the resulting disk is strongly gravitationally unstable and becomes prone to fragmentation and star formation (e.g., [233, 74]). Whether this fragmentation can be avoided is unclear. One possibility is to stabilize the disk by keeping its temperature “warm” (i.e.  $T \sim 10^4\text{K}$ , close to the virial temperature). This would fatten the disks (the scale height scales with the ratio of gas and virial temperatures); this scenario may be possible in a virtually metal-free, high redshift halo [182, 37, 288, 203].

A suite of recent numerical simulations studied gas collapse in halos with  $T_{\text{vir}} \sim 10^4\text{K}$  [217]. It was found that the gas in such halos, when collapsing in isolation, forms  $\text{H}_2$  efficiently, and (unfortunately) cools to temperatures of  $T \sim 300\text{K}$ . Although no fragmentation was seen, the cold gas (well below the virial temperature) is expected to ultimately fragment on smaller scales that have not yet been resolved [258]. More importantly, even if fragmentation was successfully avoided, there is a problem: the cold gas was found to flow inward at relatively low velocities, near the sound speed of  $\sim 2 - 3 \text{ km s}^{-1}$ , with a correspondingly low accretion rate of  $\sim 0.01 M_{\odot} \text{ yr}^{-1}$ . [217] speculate that this is explained by a series of weak shocks in the infalling gas, which prevent the gas from accelerating to large Mach numbers (this is similar to the behavior seen in three-dimensional simulations of the so-called “cold mode” of accretion in lower-redshift galaxies [131]). Ultimately, the slow infall velocities and cold temperatures produce conditions nearly identical to those in the cores of lower-mass minihalos (mentioned above); extensive ultra-high resolution simulations had concluded that the gas then forms a single  $\sim 100 M_{\odot}$  star [3, 35, 299] or perhaps fragments even further into several stars [258, 246, 77, 195], rather than forming a supermassive star or BH.

There have been at least three different ideas on how to avoid  $\text{H}_2$ -cooling and to keep the gas warm. One is for the gas to “linger” for a sufficiently long time at  $10^4\text{K}$  that it collapses to a SMBH, even before  $\text{H}_2$  has a chance to reduce the temperature ( $\text{H}_2$  is kept dissociated by collisions before the temperature falls below  $\sim 4,000\text{K}$ ). For a sufficiently high space- and column-density of neutral hydrogen, the absorption of trapped Lyman  $\alpha$  photons can be followed by collisional de-excitation, rather than the resonant scattering of the Lyman  $\alpha$  photon, effectively trapping much of the cooling radiation. This could prevent the gas temperature from falling below  $\sim 8,000\text{K}$ , and lead to such lingering and to SMBH formation – analogous to opacity-limited fragmentation in colder gas in the context of star formation [240, 210, 144].

Another possibility is that, even in the presence of significant cooling, angular momentum transport by gravitational instabilities, spiral waves, bars, etc., can drive a fraction of the gas to yet smaller scales in the galactic nucleus (e.g. [24]). Ref. [58] argued that this was particularly likely to occur in rare low angular momentum dark



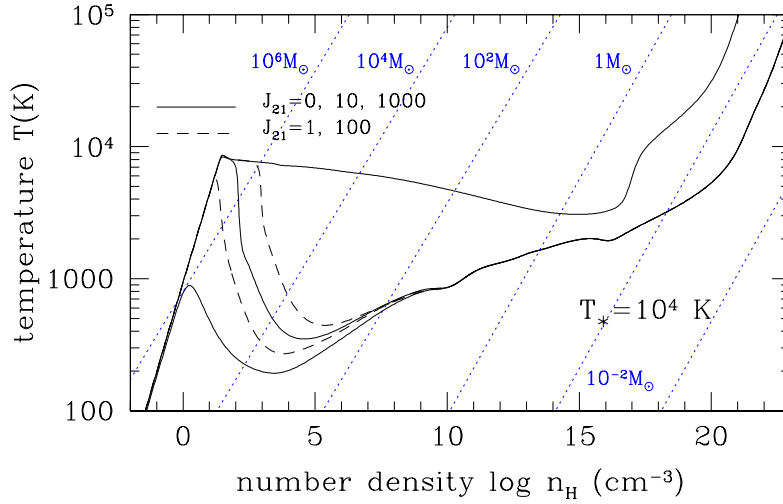


**Fig. 2** Temperature evolution of a metal-free cloud, irradiated by a strong UV flux. The models solve for the chemical and thermal evolution, but assume a pre-imposed density evolution, based on the spherical collapse model. Various cases are shown, with UV intensities at the Lyman limit of  $J_{21} = 0, 1, 10, 100$  and  $10^3$ , in the usual units of  $10^{-21} \text{erg cm}^{-2} \text{sr}^{-1} \text{s}^{-1} \text{Hz}^{-1}$  (solid and dashed curves; see the legend in the panel). Each blue dotted line corresponds to a different constant Jeans mass. The gas is heated adiabatically until a density of  $n \approx 10^0 - 10^2 \text{cm}^{-3}$ , at which  $\text{H}_2$ -cooling becomes efficient and cools the gas to a few  $\times 100 \text{K}$ . However, there exists a critical flux, with a value between  $J_{21} = 10^2$  and  $10^3$ , above which  $\text{H}_2$ -cooling is disabled (adapted from ref. [186]).

matter halos because the disk could viscously evolve before star formation commenced. A similar idea is that a small fraction of the gas, with low specific angular momentum, within the halo may collapse to the center without undergoing fragmentation [138, 152]. It may help that even if most of the gas is initially converted into stars, stellar winds and supernovae will eject a significant amount of this gas back into the nucleus; some of this gas can eventually collapse to smaller scales [22].

Finally,  $\text{H}_2$ -cooling may be disabled if the gas is exposed to a sufficiently intense UV flux  $J$ , either directly photo-dissociating  $\text{H}_2$  (in the Lyman-Werner bands near a photon energy of  $\sim 12\text{eV}$ ) or photo-dissociating the intermediary  $\text{H}^-$  (at photon

energies  $\gtrsim 0.76\text{eV}$ ). Requiring the photo-dissociation timescale,  $t_{\text{diss}} \propto J^{-1}$ , to be shorter than the  $\text{H}_2$ -formation timescale,  $t_{\text{form}} \propto \rho^{-1}$ , generically yields a critical flux that increases linearly with density,  $J^{\text{crit}} \propto \rho$ . In low-mass minihalos, the critical flux is low,  $J^{\text{crit}} \approx 0.01 - 0.1$  [102, 154, 170, 171]<sup>4</sup>. Since the gas in halos with  $T_{\text{vir}} \gtrsim 10^4\text{K}$  can cool via atomic Lyman  $\alpha$  radiation and loose pressure support, it inevitably collapses further. As a result, in these halos, the critical flux is high,  $J^{\text{crit}} \approx 10^2 - 10^5$ , depending on the assumed spectral shape (ref. [217]; see also refs. [185, 37] who found similar, but somewhat higher values). The existence of this critical flux is illustrated in Figure 2, using a one-zone model, in which the density evolution is approximated by spherical collapse, and the gas is illuminated by a source with a black-body spectrum (with a temperature of  $T = 10^4\text{K}$ , characteristic of a normal stellar population). Figure 3 shows the radial structure of a  $10^8 M_{\odot}$  halo, at the time of its collapse, when illuminated at various intensities, taken from three-dimensional simulations with the AMR code *enzo*. These profiles clearly show that when the UV flux exceeds a critical value, the core of the halo is prevented from cooling to low temperatures.

The 3D simulations also provide an estimate of the mass of the central “object” (star or SMBH) that ultimately forms at the core of the halo, based on the measured profile of the mass accretion rate. This is illustrated in Figure 4. In particular, when the flux exceeds the critical value, and the gas remains warm, the collapse is significantly delayed. However, when the gas ultimately does collapse, it accretes toward the center at the sound speed ( $c_s \approx 10\text{km/s}$ ), leading to a mass accretion rate of  $\dot{M} \approx 1 M_{\odot} \text{yr}^{-1}$ . This is much higher than in the case of cold ( $c_s \sim 1\text{ km/s}$ ) gas in halos with efficient  $\text{H}_2$  cooling (as mentioned above, the simulations find  $\dot{M} \propto c_s^3$ , as expected in self-gravitating gas).

Importantly, the critical flux is high – likely significantly exceeding the expected level of the cosmic UV background at high redshifts. Therefore, only a small subset of all  $T_{\text{vir}} \gtrsim 10^4\text{K}$  halos, which have unusually close and bright neighbors, may see a sufficiently high flux. However, given the strong clustering of early halos, there is a sufficient number of these close halo pairs to account for the abundance of the rare  $z = 6$  quasars [51]. A more significant challenge to this idea is that in order to avoid fragmentation, the gas in these halos must also remain essentially free of any metals and dust [186]. This requirement could be difficult to reconcile with the presence of a nearby, luminous galaxies.

Finally, an important point to emphasize is that the collapsing gas is optically thick, and the critical flux  $J_{\text{crit}}$  depends crucially on the details of self-shielding of the Lyman-Werner lines of  $\text{H}_2$ . Since following radiative transfer in many dozens of lines is computationally expensive, existing works have employed various simplifying approximations. The simplest (and by far most commonly used) approach is to combine a simple power-law fitting formula,  $f_{\text{shield}} = (N_{\text{H}_2}/10^{14}\text{cm}^{-2})^{-3/4}$ , for the  $\text{H}_2$  self-shielding factor [55] with an estimate for an effective  $\text{H}_2$  column density  $N_{\text{H}_2}$  (most often equated with the product of the local density and Jeans length).

---

<sup>4</sup> Here  $J$  denotes the specific intensity just below  $13.6\text{eV}$ , in the usual  $J_{21}$  units of  $10^{-21}\text{erg cm}^{-2} \text{sr}^{-1} \text{s}^{-1} \text{Hz}^{-1}$ .

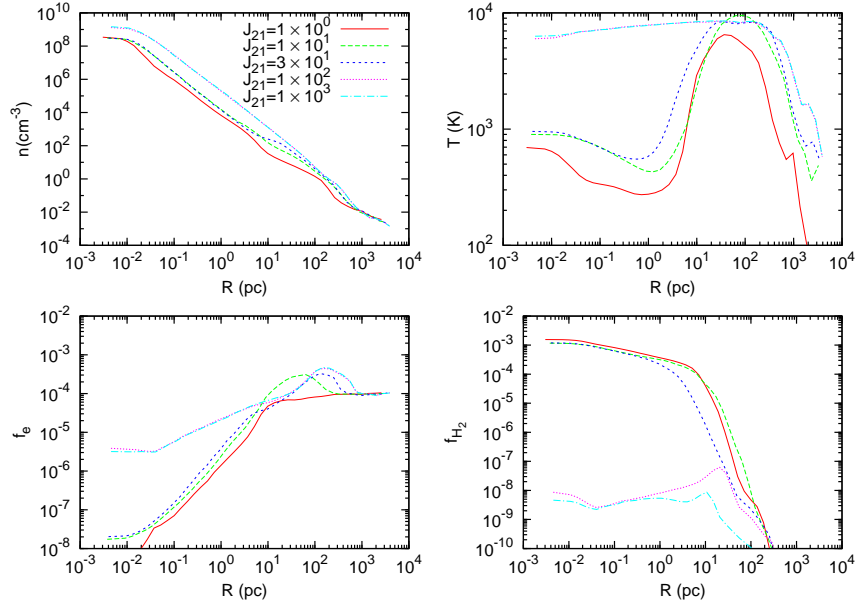


**Fig. 3** The results of adaptive mesh refinement (AMR) simulations of a primordial halo, with a total mass of a few  $\times 10^7 M_\odot$ , collapsing at redshift  $z \approx 10 - 15$ , exposed to various UV background fluxes. The four panels show snapshots of the spherically averaged profile of the particle number density, gas temperature,  $e^-$  fraction and  $H_2$  fraction, at the time of the collapse of the core, for several different values of the UV background intensity  $J_{21}$ , as labeled. The existence of a critical flux, here with a value between  $J_{21} = 30$  and  $10^2$ , above which  $H_2$ -cooling is disabled, is evident (adapted from ref. [217]).

These assumptions have recently been scrutinized in ref [289], which solved radiative line transfer exactly, using post-processing of three-dimensional simulations. This showed, rather promisingly, that when self-shielding is treated more accurately,  $J_{\text{crit}}$  is reduced by about an order of magnitude. Interestingly, this reduction comes from a product of three very different sources (each of which individually reduces the shielding by a factor of  $\sim$ two): (1) a numerical inaccuracy of the power-law  $f_{\text{shield}}$  formula, (2) the inapplicability of this fitting formula at the relevant, relatively high temperatures ( $\gtrsim 10^3 \text{K}$ ), where excited rotational levels of  $H_2$  are populated, and (3) the Jeans length yielding an overestimate of the effective average (over different sightlines) column density. The order-of-magnitude reduction in  $J$  is especially important, since the probability distribution of  $J$ , sampled by halos at  $z \gtrsim 10$ , is very steep near  $J \sim 10^4$  (see [51]). With the original high  $J_{\text{crit}}$  value, it has been shown [51] that only one in  $\approx 10^6$  halos – only those with an unusually bright and close neighbour – will see a sufficiently high flux. The reduction of the  $J_{\text{crit},21}$  value will significantly increase the number of candidates for objects that can avoid  $H_2$ -cooling and fragmentation, and makes this scenario much more viable.

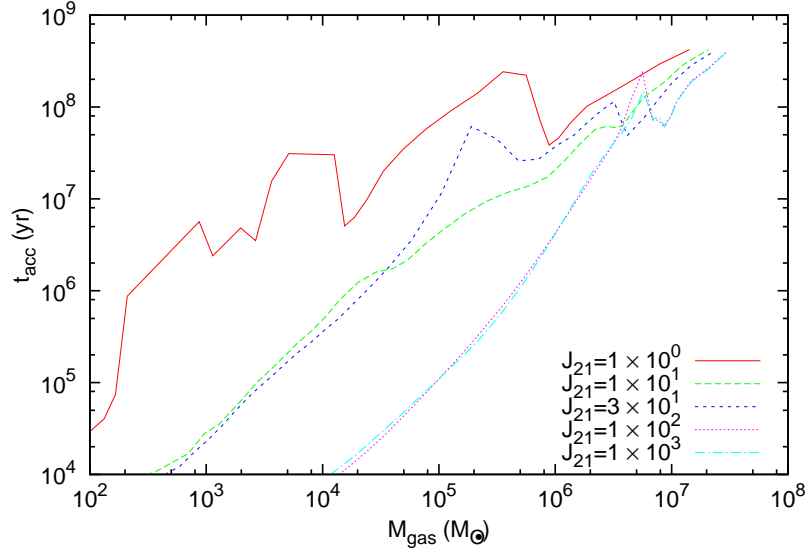


**Fig. 4** The local accretion time-scale  $t_{\text{acc}}$  as a function of the enclosed gas mass  $M_{\text{gas}}$ , in the same halo depicted in Figure 3, illuminated with different intensities, as labeled. In the halos exposed to a supercritical flux ( $J_{21} = 10^2$  and  $10^3$ ), the mass accretion rate,  $\dot{M} \approx 1 M_{\odot} \text{yr}^{-1}$ , is nearly  $10^3$  times higher than in halos whose gas cools via  $\text{H}_2$  ( $J_{21} \lesssim 10$ ). At the center of the brightly illuminated halos,  $\approx 10^5 M_{\odot}$  of gas accumulates within a Kelvin-Helmholtz time of  $\approx 10^5 M_{\odot}$ , possibly leading to the formation of a SMBH with a comparable mass (adapted from ref. [217]).

### 3.2.2 The Ultimate Fate of the Gas

Although the detailed evolutionary pathways are still not understood, a possible outcome of the above scenarios is the continued collapse of some gas to smaller scales in the galactic nucleus. As the gas flows in, it becomes optically thick, and the photon diffusion time eventually exceeds the inflow time. Radiation pressure dominates for sufficiently massive objects so that the adiabatic index is  $\Gamma \approx 4/3$ . Radiation pressure may temporarily balance gravity, forming a supermassive star or disk (SMS; e.g., [111, 277]; see, e.g., [227] for a review and additional references to earlier work). The SMS will radiate at the Eddington limit and continue contracting. When the SMS is sufficiently compact ( $GM/Rc^2 \approx 10^{-4} M_8^{-1/2}$  for non-rotating stars), general relativistic corrections to the gravitational potential become important, and the star becomes dynamically unstable because its effective polytropic index is  $\lesssim 4/3$ . For masses  $\lesssim 10^5 M_{\odot}$ , thermonuclear reactions halt the collapse and generate an explosion (e.g., [66]), but more massive objects appear to collapse directly to a SMBH (see [225] for a review; and, e.g., [231, 206] for recent simulations).

If the mass accretion rate is high ( $\sim 1 M_{\odot} \text{yr}^{-1}$ ), the outer layers of the SMS do not have time to thermally relax, and a high-pressure core-envelope structure

may develop, dubbed a “quasi-star” [25, 23, 19]. The envelope initially contains most of the mass, and the central BH embedded in the envelope can grow from this envelope; the key feature of this configuration is that the accretion is limited by the Eddington limit for the entire envelope, rather than just the BH. Interestingly, the mass accretion rate required for this model is comparable to that seen in three-dimensional simulations of  $T_{\text{vir}} \gtrsim 10^4\text{K}$  halos, *provided again that the gas in these halos can avoid  $H_2$  cooling* [217].

Finally, a possibility for the gas is to ultimately fragment into stars, but not before it reaches very high densities. If the gas is metal–enriched, this scenario may be most likely, and will result in the formation of a dense and compact stellar cluster, which naturally evolves to form a SMBH [186]. We turn to this idea in the next section.

### 3.3 The Formation of Black Holes in Stellar Clusters

The negative heat capacity of self-gravitating stellar systems makes them vulnerable to gravitational collapse in which the core of the cluster collapses on a timescale  $t_{cc}$  comparable to the two-body relaxation time of the cluster [27]. If core collapse proceeds unimpeded, the resulting high stellar densities can lead naturally to the runaway collisional growth of a single massive object which may evolve to form a black hole (as in the discussion of SMSs above). This process provides an additional route for the direct formation of SMBHs at high redshifts (or, more likely, intermediate mass seeds).

Early work suggested that the fate of stellar clusters depends sensitively on the number of stars in the cluster. [147] and [198] found that very dense massive star clusters ( $N \gtrsim 10^6 - 10^7$  stars) were required to have successful core collapse and runaway growth of a single massive object. In less massive clusters, core collapse was halted by binary heating, in which the cluster gains energy at the expense of binaries via three-body interactions [107, 113]. Successful core collapse also requires that  $t_{cc}$  is shorter than the timescale for the most massive stars to evolve off the main sequence ([199]; this requirement implies compact clusters  $\lesssim 1$  pc in size). Otherwise, mass loss from evolved stars and supernovae prevents the core from collapsing (in much the same way as binary star systems can become unbound by supernovae). In principle, massive stars could evolve into stellar-mass BHs and form a dense cluster of stellar-mass BHs. In the context of high-redshift halo formation, this is naturally expected [157], given that the first stars in the first minihalos are believed to be massive. A dense cluster of stellar-mass BHs can, in principle, grow into a more massive IMBH by coalescence due to gravitational radiation; however, this process is effective only in large stellar systems that are found in present-day galactic nuclei [184].

If the required number of stars was indeed as large as  $N \gtrsim 10^6 - 10^7$ , this would be bad news for early SMBH formation: in the cosmological hierarchy,  $\gtrsim 10^8 M_{\odot}$  halos – the smallest that could plausibly harbor such star clusters – are very rare ( $\gtrsim 2.5\sigma$  fluctuations) at  $z \gtrsim 10$ . However, recent work has revived earlier ideas

that stellar clusters are subject to a “mass segregation instability” that makes even the relatively less massive clusters prone to forming black holes ([241, 270, 22]). Because massive stars in a cluster sink by dynamical friction toward the center (mass segregation), they invariably dominate the dynamics of the cluster core and can undergo core collapse on a timescale much shorter than that of the cluster as a whole (and on a timescale shorter than their main sequence lifetime). [192] showed with N-body simulations that the resulting core collapse likely leads to runaway merger and formation of a single black hole, and [83] reached a similar conclusion for much larger  $N \sim 10^7$  using Monte Carlo simulations. Including an explicit treatment of stellar collisions, the most recent Monte-Carlo simulations find that the central massive object that forms in core has a mass of  $\sim 10^{-3}$  of the whole cluster [75].

In the context of high-redshift BH formation, [186] considered the cooling properties of gas in  $T_{\text{vir}} \gtrsim 10^4 \text{K}$  halos. It is expected that the majority of such halos, when they are assembled, had already undergone some amount of star-formation. In this case, their gas would have at least a trace amount of metals. [186] considered the case when such mildly polluted halos are exposed to a large UV flux, which dissociates  $\text{H}_2$ , and initially prevents cooling. This allows the gas to contract to very high densities, without fragmenting initially. By following the thermal and chemical evolution of such low-metallicity gas, exposed to extremely strong UV radiation, [186] found, however, that eventually, gas fragmentation is inevitable above a critical metallicity, whose value is between  $Z_{\text{cr}} \approx 3 \times 10^{-4} Z_{\odot}$  (in the absence of dust) and as low as  $Z_{\text{cr}} \approx 5 \times 10^{-6} Z_{\odot}$  (with a dust-to-gas mass ratio of about  $0.01 Z/Z_{\odot}$ ). When the metallicity exceeds these critical values, an ultra-dense cluster (the density at the time of fragmentation is  $n \gtrsim 10^{10} \text{cm}^{-3}$ ) of low-mass stars may form at the halo nucleus ([44] and [49] argued for similar scenarios, in the central regions of a protogalactic disk). Relatively massive stars in such a cluster can then rapidly coalesce into a single more massive object, which may produce an intermediate-mass BH remnant with a mass up to  $M \lesssim 10^3 M_{\odot}$ .

The above processes provide a promising channel for the formation of IMBH seeds, which can grow via mergers and/or accretion to form SMBHs. For example, [272] and [116] have incorporated such early black hole seeds into Monte Carlo simulations of the black hole merger histories. With reasonable prescriptions for the merging and accretion of black holes inside dark halos, these models can account for the observed evolution of the quasar luminosity functions at  $z < 5$  and can serve for physically motivated extrapolations to high redshifts to describe the first AGN.

It should be noted that there exist some observational evidence for IMBHs in the local universe. In particular, the presence of IMBHs with masses of order  $\sim 10^4 M_{\odot}$  are inferred from stellar kinematics in the globular clusters G1 ([71]; note that the velocity dispersion profile itself does not require a BH [15] and the evidence comes from higher-order moments of the velocity distribution [72] instead),  $\omega$  Cen [180] and in M15 ([263], although this object can also be modeled without an IMBH; [262]). Ultra-luminous X-ray sources in nearby galaxies (e.g., [45, 124, 172, 63]) have also been interpreted as accreting IMBHs. While there are viable non-IMBH interpretations of these sources (e.g., [132, 18]), the X-ray spectrum of one such source during the peak of an outburst implies the presence of a  $\gtrsim 2000 M_{\odot}$  IMBH

(assuming that the luminosity is limited to  $0.3 \times L_{\text{Edd}}$  as in stellar-mass BH X-ray binaries in their hard state; [123]).

### 3.4 Alternative Models

Since both of the “standard” scenarios discussed above require some optimistic assumptions, it is interesting to consider some more exotic possibilities.

It is commonly believed that the magnetic fields permeating galaxies such as the Milky Way arose by the amplification of a much weaker large-scale seed field. Weak primordial magnetic fields, with strengths of up to  $\sim 1\text{nG}$ , can be produced in phase transitions in the early universe, during inflation, or during the electroweak or QCD phase transitions. It has recently been shown that such a primordial magnetic field could produce a variant of the “direct collapse” scenario [215]. In particular, if the field is tangled, then ambipolar diffusion will provide an efficient new mechanism to heat the gas as it collapses in protogalactic halos. If the field has a strength above  $|B| \gtrsim 3$  (comoving) nG, the collapsing gas is kept warm ( $T \sim 10^4\text{K}$ ) until it reaches the critical density  $n_{\text{crit}} \approx 10^3\text{cm}^{-3}$  at which the roto-vibrational states of  $\text{H}_2$  approach local thermodynamic equilibrium. This is illustrated explicitly by the thermal evolution of fluid elements shown in Figure 5.  $\text{H}_2$ -cooling then remains inefficient, and the gas temperature stays near  $\sim 10^4\text{K}$ , even as it continues to collapse to higher densities. The critical magnetic field strength required to permanently suppress  $\text{H}_2$ -cooling is somewhat higher than upper limit of  $\sim 2\text{nG}$  from the cosmic microwave background (CMB). However, it can be realized in the rare  $\gtrsim (2-3)\sigma$  regions of the spatially fluctuating  $B$ -field; these regions contain a sufficient number of halos to account for the  $z \approx 6$  quasar BHs<sup>5</sup>

Another “exotic” idea is that the first PopIII stars may be powered by heating by dark matter annihilation, rather than by nuclear fusion [243]. Weakly interacting massive particles (WIMPs), can be such a heat source, as long as they reach sufficiently high density inside the first stars, and if the annihilation products are trapped inside the star. Several authors have studied the impact of this additional heating mechanism on the structure and evolution of such “dark stars” [242, 115, 297, 252, 261, 242, 65, 205]. In particular, these stars can live much longer than “normal” PopIII stars, and because their radiation is soft, they can continue to accrete gas, as long as the dark matter heating persists, and grow to masses of up to  $\sim 10^5 M_{\odot}$ . In fact, one of the challenges in these models is to explain why and how the growth of the star stops [261, 65]. An interesting prediction is that these stars are bright, and should be detectable directly by *JWST* [65].

---

<sup>5</sup> Because of the high magnetic Jeans mass, the magnetic pressure has significant dynamical effects, and can prevent gas collapse in halos with masses up to  $M \gtrsim \text{few} \times 10^{10} M_{\odot}$ . These are  $\sim 100$  times more massive than the DM halos in the “usual” direct collapse models discussed in § 3.2 above.



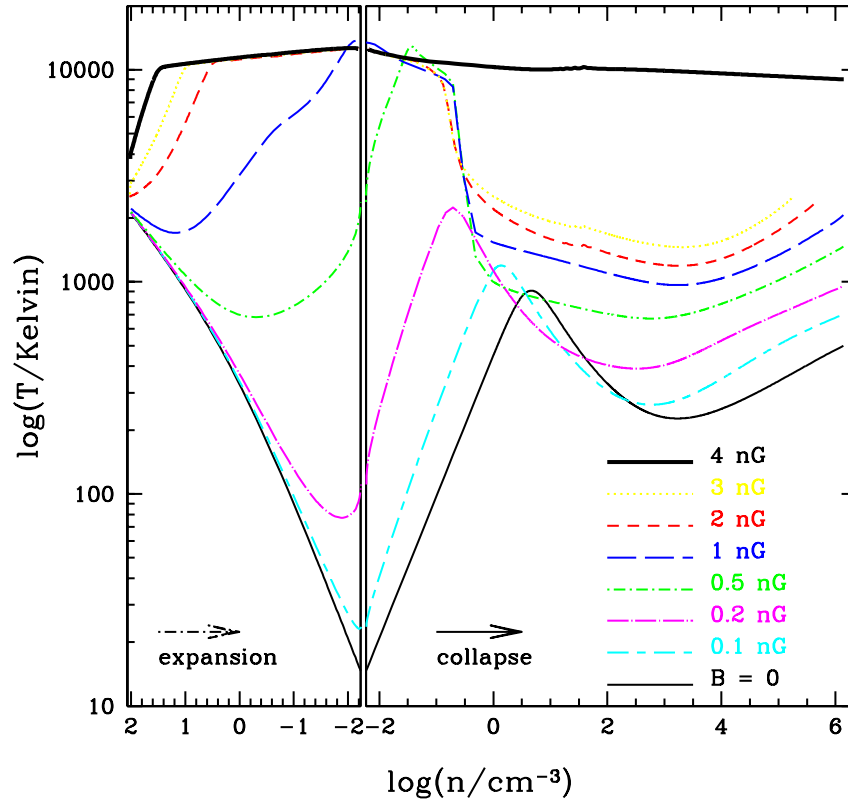


**Fig. 5** The temperature evolution of a patch of the intergalactic medium is shown as it initially expands and then turns around and collapses to high density. The different curves correspond to different values of the assumed primordial magnetic field, as labeled. The gas evolves from the left to the right on this figure. The left panel shows the expanding phase, starting from an initial density of  $\approx 100 \text{ cm}^{-3}$  (corresponding to the mean density at redshift  $z \simeq 800$ ) and ending at the turnaround just below  $n = 10^{-2} \text{ cm}^{-3}$ . The right panel follows the subsequent temperature evolution in the collapsing phase. The figure shows the existence of a critical magnetic field, with a value between  $B = 3$  and  $4 \text{ nG}$ , above which  $\text{H}_2$ -cooling is disabled, and the gas temperature always remains near  $10^4 \text{ K}$  (adapted from ref. [215]).

## 4 Observational Considerations

In this section, we first review several recent observations and their implications for the formation of black holes at high redshifts. We then then speculate on how future observations may probe the assembly of high- $z$  SMBHs.

### 4.1 Surveys for High Redshift Quasars

The majority of the  $\sim 40$  quasars known at  $z \sim 6$  to date have been discovered in the SDSS. This is perhaps somewhat surprising, since the SDSS is a relatively shallow survey (with a magnitude limit of  $i \sim 22$ ) capable of detecting only the rarest bright quasars at redshifts as high as  $z \sim 6$ . Nevertheless, the large solid angle searched for high redshift quasars ( $\sim 8,000$  square degrees) has yielded many such objects [61]. Somewhat deeper surveys covering smaller areas (a few  $\sim 100$  square degrees), such as the SDSS Deep Stripe [119], and the CFHQS [284] and UKIDSS [146] surveys, have yielded many additional detections. The most important properties (for our purposes) of these sources are that they are probably powered by SMBHs as large as a few  $\times 10^9 M_\odot$  and overall, they appear to be indistinguishable from bright quasars at moderate ( $z \sim 2 - 3$ ) redshifts, with similar spectra and inferred metallicities (e.g. [121]). In addition, a large reservoir of molecular gas is already present, even in the most distant sources [278, 279, 280].

Despite the overall similarities, there are some tentative distinctions between these  $z \gtrsim 6$  quasars and their  $z \sim 2 - 3$  counterparts. First, there is evidence for increasing Eddington ratios toward high redshift (see below). Second, quasar clustering has been found to strongly increase with redshift [229]. The observed clustering strength can be used to infer to quasar lifetimes [93, 161], and implies that the duty cycle of bright quasar activity increases significantly toward high redshifts, to near unity by  $z \approx 6$  [220]. Finally, two of the  $\sim 6$  quasars have no detectable emission from hot dust [120]. There are no known examples for such apparently hot-dust-free quasars at low redshift; this result therefore suggests that at least these two quasar BHs may have been caught at a young age of the evolution of their host galaxies (i.e., there was insufficient time for a dusty torus to form in the nucleus).

With these exceptions, the high- $z$  SMBHs and their surroundings appear as “fully developed” as their lower redshift counterparts, despite the young age ( $\lesssim 10^9$  years) of the universe at  $z \gtrsim 6$ . These rare quasars are likely harbored by massive ( $\sim 10^{12-13} M_\odot$ ) dark matter halos that form out of  $4 - 5\sigma$  peaks of the fluctuating primordial density field. The large halo mass follows directly from the space density of these sources ([99]; another method to confirm the large halo masses is to study the expected Lyman  $\alpha$  absorption signatures of cosmological gas infall onto such massive halos, as proposed by [37]). Indeed, the environment and dynamical history of an individual massive dark matter halo at  $z \sim 6$  and  $z \sim 3$  can be similar; it is their abundance that evolves strongly with cosmic epoch. This is broadly consistent with the observations: the bright  $z \sim 6$  quasars look similar to their  $z \sim 3$  counterparts, but their abundance is much reduced (by a factor of  $\sim 40$ ).

The fact that these quasars are so rare has important implications. First, they are likely to be the “tip of the iceberg” and accompanied by much more numerous populations of fainter quasars at  $z \gtrsim 6$ . The slope of the luminosity function is expected to be very steep at  $i \sim 22$ , and so pushing the magnitude limits further in future surveys should prove rewarding. The most direct constraints on this slope are from combining the CFHQS sample with the more luminous SDSS sample (yielding a total of

40 quasars between redshifts  $5.74 < z < 6.42$ ; [284]), and from gravitational lensing [46, 292, 293, 204]. Combining source counts and lensing yields the strongest limit of  $-d \log \Phi / d \log L \lesssim 3$  [291]. Second, the steep slope of the dark halo mass function implies that the masses of the host halos can be “measured” from the abundance quite accurately (see discussion in § 4.2). Conversely, since small changes in the assumed host halo mass results in large changes in the predicted abundance, large uncertainties will remain in other model parameters. In this sense, fainter, but more numerous quasars (or lack thereof) can have more constraining power for models that relate quasars to dark halos.

The most striking feature of the SDSS quasars, however, is the large black hole mass already present at  $z \sim 6$ . In the rest of this section, we critically assess whether the inferred large black hole masses are robust.

The masses of the black holes powering the SDSS quasars are inferred by assuming that (1) they shine at the Eddington luminosity with a bolometric correction identical to that of lower redshift quasars (this is justified by their similar spectra), and (2) they are neither beamed nor gravitationally lensed (both of these effects would make the quasars appear brighter and allow lower BH masses). These assumptions lead to black hole masses  $M_{\bullet} \approx (2 - 6) \times 10^9 M_{\odot}$  for the  $z > 6$  quasars known to date. These are reasonable assumptions, which have some empirical justification.

The hypothesis that the quasars are strongly beamed can be ruled out based on their line/continuum ratio. If the quasar’s emission was beamed into a solid angle covering a fraction,  $f$ , of  $4\pi$ , it would only excite emission lines within this cone, reducing the apparent line/continuum ratio by a factor  $f$ . However, the SDSS quasars have strong lines. [90] found that the line/continuum ratio of the  $z = 6.28$  quasar SDSS 1030+0524 is about twice that of the median value in the SDSS sample at  $z > 2.25$  [264]. This argument, applied to the Mg II line of the  $z = 6.41$  quasar SDSS J1148+5251 [285] yields a similar conclusion.

Another important uncertainty regarding the inferred black hole masses is whether the SDSS quasars may be strongly magnified by gravitational lensing. The optical depth to strong lensing along a random line of sight to  $z \sim 6$  is small ( $\sim 10^{-3}$ ; e.g., [134, 14]). Nevertheless, magnification bias can significantly boost the probability of strong lensing. If the intrinsic (unlensed) luminosity function at  $z \sim 6$  is steep and/or extends to faint magnitudes, then the probability of strong lensing for the SDSS quasars could be of order unity [46, 292, 293]). The overwhelming majority (more than 90%) of strong lensing events would be expected to show up as multiple images with separations at least as large as  $0.3''$ . It is difficult to produce strong magnification without such multiple images, even in non-standard lensing models (allowing ellipticity and/or external shear [130]). However, deep optical observations (e.g. with the *Hubble Space Telescope*) of the highest redshift quasars show no signs of multiple images for any of the  $z \gtrsim 6$  sources down to an angle of  $0.3''$  [204, 286].<sup>6</sup>

---

<sup>6</sup> The highest-redshift known lensed quasar is at  $z = 4.8$  and was discovered serendipitously in SDSS, initially flagged as a galaxy due to the strong blending of one of the quasar images with a bright galaxy [164].

Finally, whether or not the SDSS quasars are shining at the Eddington limit is difficult to decide empirically. Several authors [285, 267, 121, 140, 268, 269, 139, 283] have estimated Eddington ratios in samples of high redshift quasars, using observed correlations between the size of the broad line region and the luminosity of the quasar (the correlation is calibrated using reverberation mapping of lower redshift objects; e.g. [128, 266, 136]). Values range from  $\approx 0.1$  to  $\gtrsim 1$ ; in particular,  $L/L_{Edd}$  is typically found to increase with redshift, and approaches unity for the  $z \gtrsim 6$  quasars.

Inferences about Eddington ratios at high redshifts can also be made by utilizing models of the quasar population as a whole. Such models typically assume the Eddington luminosity at higher redshifts, where fuel is thought to be readily available [239, 85]. Numerous semi-analytic models for the quasar population (see, e.g., ref. [218] and references therein) have found that Eddington ratios of order unity during most of the growth of the black hole mass also yield a total remnant SMBH space density at  $z = 0$  that is consistent with observations. Ref. [43], and, more recently, [173] have self-consistently modeled accretion and radiative feedback onto an individual quasar BH, and found that (provided fuel is available) the luminosity is near the Eddington value during the phases when the quasar is on. Despite these arguments, one cannot directly rule out the possibility that the SDSS quasars shine at super-Eddington luminosities (theoretically, this is possible, as discussed above). We emphasize that if this were true and the masses were lower than  $10^9 M_\odot$ , then the SDSS quasars would have to be luminous for only a short time: maintaining the observed luminosities for  $\gtrsim 10^7$  years with a radiative efficiency of  $\epsilon \equiv L/\dot{m}c^2 = 0.1$  would bring the black hole masses up to values of  $10^9 M_\odot$  anyway.

## 4.2 Local Black Holes as Fossils

As mentioned above, SMBHs appear ubiquitous in local galaxies, with their masses correlating with the global properties of their host spheroids. Several groups have noted the broad natural implication that the formation of the SMBHs and their host spheroids must be tightly linked (see, e.g., [218]). Various independent lines of evidence suggest that spheroids are assembled at high redshifts ( $z \sim 2$ ; see [39] for the age determinations from the Sloan sample and references to older work), which would be consistent with most of the SMBH mass being accreted around this redshift (coinciding with the peak of the activity of luminous quasars). Indeed, starting from the age distribution of local early-type Galaxies, one can reconstruct the cosmic evolution of the quasar luminosity function to within observational errors, using the most naive set of assumptions (namely that the formation of stars and the assembly of the nuclear SMBHs track one another, with the SMBH radiating at a constant  $f_{Edd} \sim 0.3$ , and that the  $M_\bullet - \sigma$  correlation does not evolve with redshift [94, 219]).

This then has the unwelcome (but unsurprising) implication that the local SMBHs may contain little direct evidence of the formation of their seeds at  $z > 6$ . Indeed, it seems most plausible that the observed tight correlations, such as between  $M_\bullet$

and  $\sigma$ , are established by a feedback process which operates when most of the black hole mass is assembled. However, an upside of this hypothesis is that—with the identification of a specific feedback mechanism—physically motivated extrapolations can be made toward high redshifts. Also, while relative massive local SMBHs ( $\sim 10^9 M_\odot$ ) have undergone many mergers, those with the lowest masses ( $\sim 10^6 M_\odot$ ) are more likely to have avoided mergers. Therefore, the low-mass end of the  $M_\bullet - \sigma$  relation could be a probe of high- $z$  SMBH formation models. To be more explicit: if only a small fraction of high- $z$  halos are seeded with BHs, massive galaxies will have undergone many mergers, and will have a nuclear SMBH at present (i.e.  $f_{\text{seed}} \approx 1$ ). On the other hand, many low-mass galaxies may still have no BHs and thus the dwarf-galaxy population can have  $f_{\text{seed}} \ll 1$  [167]. Likewise, the direct-collapse models produce SMBHs whose masses are initially well above the  $M_\bullet - \sigma$  relation, which can be a diagnostic of such models [250]. Such an 'upward curvature in the low-mass end of the relation could indeed be preserved all the way down to  $z = 0$  [274].

More generally, whether the local  $M_\bullet - \sigma$  relation holds at higher redshifts, both in normalization and in slope (as discussed by several authors), and also in range (which has received less attention, but see [179]), are interesting observational questions. The highest redshift SDSS quasars do appear to satisfy the  $M_\bullet - \sigma$  relation of the local SMBHs, at least approximately. If  $M_\bullet$  is estimated assuming the Eddington luminosity, and  $\sigma$  from the CO line-width, then, at a given  $\sigma$ , high- $z$  quasars have BH masses a factor of  $\sim 4$  larger than local galaxies, although this could still be partly caused by selection (with high- $z$  quasars preferentially viewed face-on) [109] and by the observations probing a smaller (inner) fraction of the DM halo. We also note that if  $\sigma$  is estimated from the circular velocity of the host dark matter halos with the right space density (e.g., [99]), then the SDSS quasars are within the scatter of the  $M_\bullet - \sigma$  relations of [70] and also of [64]. As explained in § 4.1, the halo mass inference is reasonable. The determination of the halo mass and circular velocity from the observed abundance of quasars is also more robust than it may at first appear. This is because, despite the dependence on the poorly known duty cycle, the halo mass function is exponentially steep for the massive  $M \sim 10^{13} M_\odot$  halos at  $z \sim 6$ ; therefore, the dependence of the inferred halo mass on the duty cycle (and other uncertainties in the estimated halo abundance) is only logarithmic. The weakest link in the argument is associating the spheroid velocity dispersion with the circular velocity of the dark matter halo. There is evidence [64] of a correlation between  $M_\bullet$  and  $\sigma$ , with the velocity dispersion measured in the dark matter dominated region of SMBH host galaxies; this establishes a direct link to the dark halo and puts the above argument on somewhat firmer ground (although there are still large errors in the inferred correlation, depending on the halo profile one adopts to convert the measured circular velocity to total halo mass).

The (tentative) evidence that high-redshift AGN do not strongly deviate from the local  $M_\bullet - \sigma$  relation further supports the idea that the formation of SMBHs and their host galaxies must be tightly coupled by cosmology-independent physical processes (since the SDSS quasars are the rare peaks that have already formed at  $z \sim 6$  instead of at  $z \sim 2$ ). Besides the slope and normalization of the  $M_\bullet - \sigma$

relation, the *range* (of masses and velocity dispersions) over which observed galaxies satisfy this relation has to match up between low and high redshifts. In particular, the largest black holes observed at high redshifts have inferred masses approaching  $M_{\bullet} \sim 10^{10} M_{\odot}$ . These should also exist at low redshifts, but have not yet been discovered. In the SDSS, the galaxy with the velocity dispersion record has  $\sigma = 444 \text{ km s}^{-1}$  [208]), whereas a naive application of the local  $M_{\bullet} - \sigma$  relation would predict the presence of  $\sigma > 700 \text{ km s}^{-1}$  galaxies [179]. This puzzle is alleviated somewhat by the scatter in the relation; it is likely fully resolved by the realization that the  $M_{\bullet} - \sigma$  relation has ‘curvature’, with BHs in the largest galaxies preferentially more massive than the power-law  $M_{\bullet} - \sigma$  relation would predict [145].

There have been several suggestions in the literature for the nature of the dynamical coupling between the formation of the black hole and its spheroid host. The most promising is radiative or mechanical feedback from the SMBH on the gas supply in the bulge. The essential idea (going back to [236]) is that when the black hole in the center of the galaxy grows too large, its outflows and radiation unbind the gas in the bulge or in the disk, quenching further black hole growth via accretion and further star formation. Competition with star formation for the gas supply may also play a role [50, 149]. Note that these mechanisms can readily work at any redshift.

There are several alternative possibilities for the origin of the  $M_{\bullet} - \sigma$  relation, which include: (1) filling the dark matter loss cone [188]. In this model, the growth of the SMBH occurs first through the accretion of collisional dark matter particles, and subsequently through the scattering of these particles into orbits that are then perturbed to pass sufficiently close to the black hole’s Schwarzschild radius to be captured. This model runs into difficulties with the so-called Sofyan argument; since the SMBHs are fed mostly dark matter rather than gas, there is no associated radiation. (2) Direct capture of stars on high eccentricity orbits by the SMBH [306, 169]. This model has a similar problem because black holes more massive than  $\gtrsim 10^8 M_{\odot}$  do not tidally disrupt stars, so there is again no radiative output associated with the black hole growth. (3) Stellar captures by the accretion disk feeding the hole [175].

Solving the puzzle of the origin of the  $M_{\bullet} - \sigma$  relation will have important implications for high- $z$  SMBHs: in particular, it will generally determine how the relation evolves with redshift.

### 4.3 The Future

In this section, we briefly summarize the possibility of probing the continuum and line emission from AGN beyond the current redshift horizon of  $z \sim 6$ . This discussion is necessarily based on models for how the BH population evolves at  $z > 6$ . Such models can be constructed by assuming that SMBHs populate dark matter halos, e.g., in accordance with the locally measured  $M_{\bullet} - \sigma$  relation (or an extrapolation of the relation to higher redshifts). The relation appears to hold, at least to within a factor of a few, for  $z \sim 3$  quasars (this is based on using the  $H\beta/OIII$  lines

as proxies for black hole mass and  $\sigma$ , respectively; e.g., [232]), and also at  $z \sim 6$  (see § 4.1). No doubt the observational constraints will improve as both black hole masses and velocity dispersions are measured in larger samples of distant quasars. Correspondingly, extrapolations to high redshifts will be more reliable as the feedback processes that regulate black hole growth are better understood. Here we summarize predictions from the simplest models.

### 4.3.1 Broadband Detections

Predictions for the number counts of high redshift AGN have been made using simple semi-analytic models for the near-infrared [96] and in the soft X-rays [98]. In these early models, the quasar black hole was assumed to have a fixed fraction  $\sim 10^{-4}$  of the halo mass, shine at the Eddington luminosity, and have a duty cycle of bright activity of  $t_q \sim 10^6$  years.

In such models, the surface density of sources is very high in the optical/near-infrared bands, even at  $z \sim 10$ . For example, in the  $1 - 5 \mu\text{m}$  band, the  $\sim 1 \text{ nJy}$  sensitivity of the *James Webb Space Telescope (JWST)* will allow the detection of an  $\sim 10^5 M_\odot$  black hole at  $z = 10$  (provided that the black hole shines at the Eddington limit with a standard template spectrum [59]). Surface densities as high as several sources per square arcminute are predicted at this threshold from  $z \gtrsim 5$ , with most of these sources at  $z \gtrsim 10$  [97]. We note, however, that these predictions are very sensitive to the assumed duty cycle of bright activity. For example, for  $t_q \sim 10^7$  years, or  $M_\bullet \propto M_{\text{halo}}^{5/3}$ , the  $z \sim 10$  counts can be smaller by a factor of 10-100 (depending on what redshift-dependence is assumed for the above scaling relation between black hole and halo mass at high redshift; see [96, 84, 295] for related discussion). It would also be interesting to detect the host galaxies of ultrahigh redshift AGN, which should be feasible with *JWST*'s sensitivity. If the galaxies occupy a fair fraction ( $\sim 5\%$ ) of the virial radius of their host halos, then a large fraction ( $\gtrsim 50\%$ ) of them can potentially be resolved with *JWST*'s planned angular resolution of  $\sim 0.06''$  [97, 14]. The Large Synoptic Survey Telescope (LSST<sup>7</sup>), with a planned capability of going  $\sim 5$  magnitudes deeper than SDSS in a  $\sim 3$  times larger solid angle, will be an ideal instrument for studying high-redshift quasars in the optical/near-infrared.

In the soft X-rays, the  $0.5 - 2 \text{ keV}$  flux of  $2.5 \times 10^{-17} \text{ ergs cm}^{-2} \text{ s}^{-1}$  reached in a 2 Ms exposure of CDF-North [5] corresponds to a larger ( $\sim 2 \times 10^7 M_\odot$ ; see Figure 1 in [98]) black hole at  $z = 10$ , but nevertheless, thousands of sources are predicted at  $z \gtrsim 5$  per square degree, and tens per square degree at  $z > 10$ . This would imply that tens of  $z > 5$  sources should have been detectable already in the CDFs, whereas only a handful of potential candidates, and no confirmed sources, have been found. In revised models with longer quasar lifetimes and thus a steeper scaling of  $M_\bullet$  with  $M_{\text{halo}}$ , these numbers can be sharply decreased [97, 84], which can bring the expected counts into agreement with current non-detections [295].

---

<sup>7</sup> www.lsst.org



The radio sensitivity of the extended Very Large Array and other forthcoming instruments (e.g., Allen Telescope Array and Square Kilometer Array) is also promising for detecting AGN beyond  $z \sim 6$ . Using the updated scaling of black hole mass with halo mass and redshift [295] and assuming the same radio-loud fraction ( $\sim 10\%$ ) as at lower redshifts, a simple model predicts that  $\sim$ ten  $10\mu\text{Jy}$  sources per square degree should be detectable at  $1 - 10$  GHz [101]. The identification of these quasars is a challenge, but should, in principle, be feasible with deep optical/IR observations. To date, only two such radio-selected quasars have been identified (in optical follow-ups of sources in the FIRST and VLA radio catalogs; [163, 304]), which falls below the expectations from the simple model by a factor of several.

In addition to direct detection of AGN at very high redshifts, it may also be possible to detect lower mass seed black holes at comparable redshifts (or higher). In particular, a plausible model for gamma-ray bursts (GRBs) invokes accretion onto a newly formed  $\sim 10 M_{\odot}$  black hole (the collapsar model; e.g., [290]). *Swift* has now detected four bursts beyond  $z > 6$ : GRB090429B at  $z = 9.4$  [47], GRB090423 at  $z = 8.2$  [251, 207], GRB080913 at  $z = 6.7$  [79], and GRB050904 at  $z = 6.3$  [129, 104], for which the afterglow emission has also been measurable; such afterglows should remain detectable in the infrared out to  $z \sim 20$  [141, 42]. Their detection and the characterization of their spectrum and light-curve would open up a new probe of black hole formation and evolution at high redshifts.

In summary, model predictions for the continuum emission of  $z > 6$  AGN are very sensitive to how one extrapolates the  $M_{\bullet} - M_{\text{halo}}$  relation to  $z \gtrsim 6$ . However, this should be viewed as “good news”: (1) large numbers of detectable AGN at these redshifts are certainly possible, and (2) their detection will put strong constraints on models for the origin and evolution of the black hole population.

#### 4.3.2 Emission Line Measurements

The strongest recombination lines of H and He from  $5 < z < 20$  AGN will fall in the near-infrared bands of *JWST* and could be bright enough to be detectable. Specific predictions have been made for the source counts in the  $\text{H}\alpha$  emission line [181] and for the three strongest HeII lines [183, 257]. The key assumption is that most of the ionizing radiation produced by the miniquasars is processed into such recombination lines (rather than escaping into the IGM). Under this assumption, the lines are detectable for a fiducial  $10^5 M_{\odot}$  miniquasar at  $z = 10$ . The  $\text{Ly}\alpha$  line is more susceptible to absorption by neutral hydrogen in the IGM near the source but should be detectable for bright sources that are surrounded by a large enough HII region so that  $\text{Ly}\alpha$  photons shift out of resonance before hitting the neutral IGM [41]. If the Lyman  $\alpha$  emission is scattered off expanding shells of material (as expected from galactic winds), this will further shift the photons away from resonance, and make the emission line more detectable [53]. We also note that in the “trapped” Lyman  $\alpha$  model for direct collapse mentioned in § 3.2, the Lyman  $\alpha$  emission ultimately emerging from the collapsing halo (before forming the SMBH) appears detectable with *JWST*, as well – as a low-surface brightness diffuse blob [143].

The simultaneous detection of H and He lines would be especially significant. As already argued above, the hardness of the ionizing continuum from the first sources of ultraviolet radiation plays a crucial role in the reionization of the IGM. It would therefore be very interesting to directly measure the ionizing continuum of any  $z > 6$  source. While this may be feasible at X-ray energies for exceptionally bright sources, the absorption by neutral gas within the source and in the intervening IGM will render the ionizing continuum of high redshift sources inaccessible to direct observation out to  $1\mu\text{m}$ . This is a problem if the ionizing sources are black holes with  $M < 10^8 M_\odot$  at  $z \sim 10$  (easily detectable at wavelengths red-ward of redshifted Ly $\alpha$  in the near-infrared by *JWST*, but too faint to see in X-rays). The comparison of H $\alpha$  and HeII line strengths can be used to infer the ratio of HeII to HI ionizing photons,  $Q = \dot{N}_{\text{ion}}^{\text{HeII}} / \dot{N}_{\text{ion}}^{\text{HI}}$ . A measurement of this ratio would shed light on the nature of the first luminous sources, and, in particular, it could reveal if the source has a soft (stellar) or hard (AGN-like) spectrum. Note that this technique has already been successfully applied to constrain the spectra of sources in several nearby extragalactic HII regions [69]. Lyman break galaxies at  $z \approx 3$  also appear to have unusually strong (for a normal stellar population) He1640 emission line; however, the lack of X-rays rule out an AGN explanation (the observation could be explained instead by the presence of PopIII stars in these galaxies [122] or by an unusual abundant population of Wolf-Rayet stars [32] that can produce the He1640 line while avoiding an overproduction of metal lines).

Provided the gas in the high redshift AGN is enriched to near-solar levels, several molecular lines may be visible. In fact, CO has already been detected in the hosts of the most distant quasars [278, 279, 280]. The detectability of CO for high redshift sources in general has been considered in simple theoretical models [237]. If AGN activity is accompanied by a star formation rate of  $\gtrsim 30 M_\odot/\text{yr}$ , the CO lines are detectable at all redshifts  $z = 5 - 30$  by the Millimeter Array (the redshift independent sensitivity is due to the increasing CMB temperature with redshift), while the Atacama Large Millimeter Array (ALMA) could reveal even fainter CO emission, and other C and O lines in emission, providing spatially resolved images [211]. The detection of these molecular lines will provide valuable information on the stellar content and gas kinematics near the AGN.

### 4.3.3 Gravitational Waves

The most direct observational constraints on the SMBH assembly at  $z > 6$ , with especially clear distinctions between the “stellar–mass seed” and “direct-collapse” scenarios, may come from detecting the gravitational waves produced during the SMBH mergers. The *Laser Interferometer Space Antenna (LISA)* is expected to be able to detect mergers of SMBHs in the mass range  $\sim (10^4 - 10^7) M_\odot / (1 + z)$  with high S/N out to  $z \sim 30$  [12]. Binary spins and BH masses is expected to be measured with high precision up to  $z \sim 10$  [265], especially if spin precession [142] and

higher-order harmonics of the waveform [166] are included in the analysis.<sup>8</sup> Many authors have computed the expected *LISA* event rate from high-redshift SMBH merger population models in a range of plausible models. The published estimates ([167, 294, 212, 213, 117, 214, 151]; see a review in [10]), even at lower redshifts, vary by orders of magnitude, from  $\sim 1$  to as high as  $\sim 10^4 \text{ yr}^{-1}$ ; there is a large range even among models that are explicitly calibrated to fit the evolution of the quasar luminosity function [151].

Closest to the present context of the growth of SMBHs at  $z > 6$  are the Monte-Carlo merger tree models in ref. [250] (discussed in § 3.1.2 above). These models coupled the merger trees with the orbits of oscillating kicked BHs, to predict detection rates for *LISA*. They have surveyed a wide range of candidate assembly models, including those with rare, massive seeds, or through ultra-early production of numerous Pop-III remnant seeds. As mentioned above, in the latter model, seed BHs need to stop forming below a redshift  $z_{\text{cut}} \sim 20$ , in order to avoid overproducing  $10^6 M_{\odot}$  BHs.

The simplest SMBH assembly scenarios, which have constant accretion rates, but in which BH seed formation stops abruptly at some redshift, and which meet constraints at both the high-mass and low-mass end of the  $z = 6$  SMBH mass function, predict negligibly low *LISA* event rates. The reason for this pessimistic conclusion is as follows: in these models, the BHs that grow into the most massive, highest-redshift quasar-SMBHs accrete at the same (exponential) rate as all the other BHs, typically resulting in a vast overproduction of massive ( $m \sim 10^6 M_{\odot}$ ) holes. In order to offset this overproduction, seeds must be made very rare, and this diminishes the *LISA* rates. It is difficult to envision a scenario for high ( $\gtrsim 10$  per year per unit redshift) detection rates unless a vast number of SMBHs in the  $10^{5-7} M_{\odot}$  range lurk in the universe at all redshifts, which the current electromagnetic surveys have missed.

A different class of models, which successfully build the  $z \sim 6$  quasar BHs, are those in which the SMBH masses are self-regulated by internal feedback, to always maintain the  $M_{\bullet} - \sigma$  relation. These models can evade this constraint, and produce *LISA* rates as high as  $30 \text{ yr}^{-1}$ . The key difference in these models with higher *LISA* rates is that the SMBH growth is driven by a large number of seed BHs and far lower gas accretion rates than those required in the constant-accretion models. The majority of the *LISA* events occur at  $z \approx 6$  and in the low end ( $10^3 - 10^4 M_{\odot}$ ) of *LISA*'s mass range for detection.

Also, for these models, the ejected BH mass density can exceed that of the galactic BH population at  $z = 6$ . Most ejected holes are expected to have low masses (still similar to the original seed mass), but an ejected BH can be as massive as  $\sim 10^8 M_{\odot}$  if large recoil velocities are allowed (e.g. if spins are not always aligned with the orbital angular momentum of the binary).

---

<sup>8</sup> As this paper was being written, NASA announced a decision to withdraw from the *LISA* experiment. The European Space Agency is continuing to consider a redesigned version of *LISA*, with a smaller budget, and a launch date of approximately 2021-2022. Given the very high S/N ratios forecast for the original version of *LISA*, the redesigned “*LISA-lite*” mission should still be able to detect low-mass SMBHs out to high redshifts.

Using similar “merger tree” massive black hole formation models, [214] analyzed the predicted mass– and redshift–distribution of LISA events. These models have input assumptions similar to the “ $M_{\bullet} - \sigma$ ” models in [250], but with varying initial seed masses. These predict a handful of detectable events at  $z > 10$ . The raw total event rates in the two models are very similar. However, the mass-distribution of events is different (low-mass mergers are missing in the ‘heavy seed’ model). Another key diagnostic between the ‘heavy’ and ‘stellar-mass’ seed models is the mass ratio of the BHs in these detectable events: while the former models predict near-equal mass mergers, in the latter case, one of the merger partners typically have time to grow, resulting in typical mass ratios of  $q = 0.1 - 0.2$ .

It is worthwhile to note that essentially all of the work on the gravity wave signal from black hole-black hole in-spiral has assumed efficient (nearly instantaneous) mergers. Stellar-scattering and gas can help drive BHs together on large scales, which can affect detections of the most massive nearby SMBHs by Pulsar Timing Arrays [135] and extreme mass ratio inspiral events by *LISA* [303]. However, SMBH-SMBH coalescences, when they are in *LISA*’s frequency window, are well within the rapidly merging purely gravitational wave-driven regime, at least if the circumbinary gas forms a thin disk [95].

## 5 Conclusions

In this review, we have summarized theoretical ideas and observational constraints on how massive black holes form at the centers of the earliest protogalaxies, and how such black holes grow via accretion and mergers to give rise to the observed population of black holes at  $z \gtrsim 6$  and in the local and moderate redshift universe. As this review shows, this remains a poorly understood but rich and important problem. Perhaps the most direct way of probing the role of mergers in black hole assembly and evolution at  $z > 10$  is via their gravity wave signatures, which will hopefully be feasible with the redesigned version of LISA being considered by ESA.

In addition to being of intrinsic interest for understanding the AGN phenomena, sources of gravity waves, etc., there is strong evidence that the formation and evolution of black holes is coupled to the formation and evolution of the host galaxy in which the black hole resides (e.g., the  $M_{\bullet} - \sigma$  relation), and thus to the cosmological formation of nonlinear dark matter structures (i.e., the dark halos surrounding these galaxies). We anticipate that this will remain a growth area of research in the coming years, with continued rapid progress on both the observational and theoretical fronts.

**Acknowledgements** The author wishes to thank the editors of this volume for their patience during the preparation of this article. I would also like to thank my recent collaborators, especially Taka Tanaka, Cien Shang, Mark Dijkstra and Greg Bryan, whose work was especially emphasized here, and Eliot Quataert for permission to draw on material in our earlier joint review. The work described here was supported in part by the NSF, NASA, and by the Polányi Program of the Hungarian National Office for Research and Technology (NKTH).

## References

1. T. Abel, P. Anninos, Y. Zhang, and M. L. Norman. Modeling primordial gas in numerical cosmology. *New Astronomy*, 2:181–207, August 1997.
2. T. Abel, G. L. Bryan, and M. L. Norman. The Formation and Fragmentation of Primordial Molecular Clouds. *ApJ*, 540:39–44, September 2000.
3. T. Abel, G. L. Bryan, and M. L. Norman. The Formation of the First Star in the Universe. *Science*, 295:93–98, January 2002.
4. T. Abel and Z. Haiman. The Role of  $H_2$  Molecules in Cosmological Structure Formation. In F. Combes & G. Pineau Des Forets, editor, *Molecular Hydrogen in Space*, page 237, 2000.
5. D. M. Alexander, F. E. Bauer, W. N. Brandt, D. P. Schneider, A. E. Hornschemeier, C. Vignali, A. J. Barger, P. S. Broos, L. L. Cowie, G. P. Garmire, L. K. Townsley, M. W. Bautz, G. Chartas, and W. L. W. Sargent. The Chandra Deep Field North Survey. XIII. 2 Ms Point-Source Catalogs. *AJ*, 126:539–574, August 2003.
6. M. A. Alvarez, J. H. Wise, and T. Abel. Accretion onto the First Stellar-Mass Black Holes. *ApJL*, 701:L133–L137, August 2009.
7. P. Amaro-Seoane, A. Sesana, L. Hoffman, M. Benacquista, C. Eichhorn, J. Makino, and R. Spurzem. Triplets of supermassive black holes: astrophysics, gravitational waves and detection. *MNRAS*, 402:2308–2320, March 2010.
8. P. J. Armitage and P. Natarajan. Accretion during the Merger of Supermassive Black Holes. *ApJL*, 567:L9–L12, March 2002.
9. J. Arons. Photon bubbles - Overstability in a magnetized atmosphere. *ApJ*, 388:561–578, April 1992.
10. K. G. Arun, S. Babak, E. Berti, N. Cornish, C. Cutler, J. Gair, S. A. Hughes, B. R. Iyer, R. N. Lang, I. Mandel, E. K. Porter, B. S. Sathyaprakash, S. Sinha, A. M. Sintes, M. Trias, C. Van Den Broeck, and M. Volonteri. Massive black-hole binary inspirals: results from the LISA parameter estimation taskforce. *Classical and Quantum Gravity*, 26(9):094027, May 2009.
11. J. G. Baker, W. D. Boggs, J. Centrella, B. J. Kelly, S. T. McWilliams, M. C. Miller, and J. R. van Meter. Modeling Kicks from the Merger of Generic Black Hole Binaries. *ApJL*, 682:L29–L32, July 2008.
12. J. G. Baker, S. T. McWilliams, J. R. van Meter, J. Centrella, D.-I. Choi, B. J. Kelly, and M. Koppitz. Binary black hole late inspiral: Simulations for gravitational wave observations. *Phys. Rev. D*, 75(12):124024, June 2007.
13. R. Barkana, Z. Haiman, and J. P. Ostriker. Constraints on Warm Dark Matter from Cosmological Reionization. *ApJ*, 558:482–496, September 2001.
14. R. Barkana and A. Loeb. High-Redshift Galaxies: Their Predicted Size and Surface Brightness Distributions and Their Gravitational Lensing Probability. *ApJ*, 531:613–623, March 2000.
15. H. Baumgardt, J. Makino, P. Hut, S. McMillan, and S. Portegies Zwart. A Dynamical Model for the Globular Cluster G1. *ApJL*, 589:L25–L28, May 2003.
16. M. C. Begelman. Black holes in radiation-dominated gas - an analogue of the Bondi accretion problem. *MNRAS*, 184:53–67, July 1978.
17. M. C. Begelman. Super-Eddington Atmospheres That Do Not Blow Away. *ApJ*, 551:897–906, April 2001.
18. M. C. Begelman. Super-Eddington Fluxes from Thin Accretion Disks? *ApJL*, 568:L97–L100, April 2002.
19. M. C. Begelman. Evolution of supermassive stars as a pathway to black hole formation. *MNRAS*, 402:673–681, February 2010.
20. M. C. Begelman, R. D. Blandford, and M. J. Rees. Massive black hole binaries in active galactic nuclei. *Nature*, 287:307–309, September 1980.
21. M. C. Begelman and D. L. Meier. Thick accretion disks - Self-similar, supercritical models. *ApJ*, 253:873–896, February 1982.
22. M. C. Begelman and M. J. Rees. The fate of dense stellar systems. *MNRAS*, 185:847–860, December 1978.

23. M. C. Begelman, E. M. Rossi, and P. J. Armitage. Quasi-stars: accreting black holes inside massive envelopes. *MNRAS*, 387:1649–1659, July 2008.
24. M. C. Begelman and I. Shlosman. Angular Momentum Transfer and Lack of Fragmentation in Self-Gravitating Accretion Flows. *ApJL*, 702:L5–L8, September 2009.
25. M. C. Begelman, M. Volonteri, and M. J. Rees. Formation of supermassive black holes by direct collapse in pre-galactic haloes. *MNRAS*, 370:289–298, July 2006.
26. J. Binney. The physics of dissipational galaxy formation. *ApJ*, 215:483–491, July 1977.
27. J. Binney and S. Tremaine. *Galactic dynamics*. Princeton University Press, 1987.
28. O. Blaes and A. Socrates. Local Dynamical Instabilities in Magnetized, Radiation Pressure-supported Accretion Disks. *ApJ*, 553:987–998, June 2001.
29. R. D. Blandford and M. C. Begelman. On the fate of gas accreting at a low rate on to a black hole. *MNRAS*, 303:L1–L5, February 1999.
30. R. D. Blandford and M. C. Begelman. Two-dimensional adiabatic flows on to a black hole - I. Fluid accretion. *MNRAS*, 349:68–86, March 2004.
31. L. Blecha and A. Loeb. Effects of gravitational-wave recoil on the dynamics and growth of supermassive black holes. *MNRAS*, 390:1311–1325, November 2008.
32. J. Brinchmann, M. Pettini, and S. Charlot. New insights into the stellar content and physical conditions of star-forming galaxies at  $z = 2-3$  from spectral modelling. *MNRAS*, 385:769–782, April 2008.
33. J. M. Bromley, R. S. Somerville, and A. C. Fabian. High-redshift quasars and the supermassive black hole mass budget: constraints on quasar formation models. *MNRAS*, 350:456–472, May 2004.
34. V. Bromm, P. S. Coppi, and R. B. Larson. Forming the First Stars in the Universe: The Fragmentation of Primordial Gas. *ApJL*, 527:L5–L8, December 1999.
35. V. Bromm, P. S. Coppi, and R. B. Larson. The Formation of the First Stars. I. The Primordial Star-forming Cloud. *ApJ*, 564:23–51, January 2002.
36. V. Bromm, A. Ferrara, and A. Heger. *First stars: formation, evolution and feedback effects*, page 180. Cambridge University Press, January 2009.
37. V. Bromm and A. Loeb. Formation of the First Supermassive Black Holes. *ApJ*, 596:34–46, October 2003.
38. B. J. Carr, J. R. Bond, and W. D. Arnett. Cosmological consequences of Population III stars. *ApJ*, 277:445–469, February 1984.
39. A. Cattaneo and M. Bernardi. The quasar epoch and the stellar ages of early-type galaxies. *MNRAS*, 344:45–52, September 2003.
40. A. Cavaliere, R. Giacconi, and N. Menci. X-Raying the Star Formation History of the Universe. *ApJL*, 528:L77–L80, January 2000.
41. R. Cen and Z. Haiman. Quasar Strömgren Spheres Before Cosmological Reionization. *ApJL*, 542:L75–L78, October 2000.
42. B. Ciardi and A. Loeb. Expected Number and Flux Distribution of Gamma-Ray Burst Afterglows with High Redshifts. *ApJ*, 540:687–696, September 2000.
43. L. Ciotti and J. P. Ostriker. Cooling Flows and Quasars. II. Detailed Models of Feedback-modulated Accretion Flows. *ApJ*, 551:131–152, April 2001.
44. P. C. Clark, S. C. O. Glover, and R. S. Klessen. The First Stellar Cluster. *ApJ*, 672:757–764, January 2008.
45. E. J. M. Colbert and R. F. Mushotzky. The Nature of Accreting Black Holes in Nearby Galaxy Nuclei. *ApJ*, 519:89–107, July 1999.
46. J. M. Comerford, Z. Haiman, and J. Schaye. Constraining the Redshift  $z \sim 6$  Quasar Luminosity Function Using Gravitational Lensing. *ApJ*, 580:63–72, November 2002.
47. A. Cucchiara, A. J. Levan, D. B. Fox, N. R. Tanvir, T. N. Ukwatta, E. Berger, T. Krühler, A. Küpcü Yoldaş, X. F. Wu, K. Toma, J. Greiner, F. Olivares E., A. Rowlinson, L. Amati, T. Sakamoto, K. Roth, A. Stephens, A. Fritz, J. P. U. Fynbo, J. Hjorth, D. Malesani, P. Jakobsson, K. Wiersema, P. T. O’Brien, A. M. Soderberg, R. J. Foley, A. S. Fruchter, J. Rhoads, R. E. Rutledge, B. P. Schmidt, M. A. Dopita, P. Podsiadlowski, R. Willingale, C. Wolf, S. R. Kulkarni, and P. D’Avanzo. A Photometric Redshift of  $z \sim 9.4$  for GRB 090429B. *ArXiv e-prints*, May 2011.



48. N. Dalal, U.-L. Pen, and U. Seljak. Large-scale BAO signatures of the smallest galaxies. *JCAP*, 11:7, November 2010.
49. B. Devecchi and M. Volonteri. Formation of the First Nuclear Clusters and Massive Black Holes at High Redshift. *ApJ*, 694:302–313, March 2009.
50. T. Di Matteo, R. A. C. Croft, V. Springel, and L. Hernquist. Black Hole Growth and Activity in a  $\Lambda$  Cold Dark Matter Universe. *ApJ*, 593:56–68, August 2003.
51. M. Dijkstra, Z. Haiman, A. Mesinger, and J. S. B. Wyithe. Fluctuations in the high-redshift Lyman-Werner background: close halo pairs as the origin of supermassive black holes. *MNRAS*, 391:1961–1972, December 2008.
52. M. Dijkstra, Z. Haiman, M. J. Rees, and D. H. Weinberg. Photoionization Feedback in Low-Mass Galaxies at High Redshift. *ApJ*, 601:666–675, February 2004.
53. M. Dijkstra and J. S. B. Wyithe. Seeing through the trough: outflows and the detectability of Ly $\alpha$  emission from the first galaxies. *MNRAS*, 408:352–361, October 2010.
54. C. Dotan and N. J. Shaviv. Super-Eddington slim accretion discs with winds. *MNRAS*, 413:1623–1632, May 2011.
55. B. T. Draine and F. Bertoldi. Structure of Stationary Photodissociation Fronts. *ApJ*, 468:269, September 1996.
56. G. Efstathiou. Suppressing the formation of dwarf galaxies via photoionization. *MNRAS*, 256:43P–47P, May 1992.
57. G. Efstathiou and M. J. Rees. High-redshift quasars in the Cold Dark Matter cosmogony. *MNRAS*, 230:5P, February 1988.
58. D. J. Eisenstein and A. Loeb. Origin of quasar progenitors from the collapse of low-spin cosmological perturbations. *ApJ*, 443:11–17, April 1995.
59. M. Elvis, B. J. Wilkes, J. C. McDowell, R. F. Green, J. Bechtold, S. P. Willner, M. S. Oey, E. Polonski, and R. Cutri. Atlas of quasar energy distributions. *ApJS*, 95:1–68, November 1994.
60. A. Escala, R. B. Larson, P. S. Coppi, and D. Mardones. The Role of Gas in the Merging of Massive Black Holes in Galactic Nuclei. II. Black Hole Merging in a Nuclear Gas Disk. *ApJ*, 630:152–166, September 2005.
61. X. Fan. Evolution of high-redshift quasars. *New Astronomy Review*, 50:665–671, November 2006.
62. X. Fan, M. A. Strauss, D. P. Schneider, R. H. Becker, R. L. White, Z. Haiman, M. Gregg, L. Pentericci, E. K. Grebel, V. K. Narayanan, Y.-S. Loh, G. T. Richards, J. E. Gunn, R. H. Lupton, G. R. Knapp, Ž. Ivezić, W. N. Brandt, M. Collinge, L. Hao, D. Harbeck, F. Prada, J. Schaye, I. Strateva, N. Zakamska, S. Anderson, J. Brinkmann, N. A. Bahcall, D. Q. Lamb, S. Okamura, A. Szalay, and D. G. York. A Survey of  $z > 5.7$  Quasars in the Sloan Digital Sky Survey. II. Discovery of Three Additional Quasars at  $z > 6$ . *AJ*, 125:1649–1659, April 2003.
63. S. A. Farrell, N. A. Webb, D. Barret, O. Godet, and J. M. Rodrigues. An intermediate-mass black hole of over 500 solar masses in the galaxy ESO243-49. *Nature*, 460:73–75, July 2009.
64. L. Ferrarese. Beyond the Bulge: A Fundamental Relation between Supermassive Black Holes and Dark Matter Halos. *ApJ*, 578:90–97, October 2002.
65. K. Freese, C. Ilie, D. Spolyar, M. Valluri, and P. Bodenheimer. Supermassive Dark Stars: Detectable in JWST. *ApJ*, 716:1397–1407, June 2010.
66. G. M. Fuller, S. E. Woosley, and T. A. Weaver. The evolution of radiation-dominated stars. I - Nonrotating supermassive stars. *ApJ*, 307:675–686, August 1986.
67. D. Galli and F. Palla. The chemistry of the early Universe. *A&A*, 335:403–420, July 1998.
68. C. F. Gammie. Photon bubbles in accretion discs. *MNRAS*, 297:929–935, July 1998.
69. D. R. Garnett, R. C. Kennicutt, Jr., Y.-H. Chu, and E. D. Skillman. He II emission in extragalactic H II regions. *ApJ*, 373:458–464, June 1991.
70. K. Gebhardt, R. Bender, G. Bower, A. Dressler, S. M. Faber, A. V. Filippenko, R. Green, C. Grillmair, L. C. Ho, J. Kormendy, T. R. Lauer, J. Magorrian, J. Pinkney, D. Richstone, and S. Tremaine. A Relationship between Nuclear Black Hole Mass and Galaxy Velocity Dispersion. *ApJL*, 539:L13–L16, August 2000.



71. K. Gebhardt, R. M. Rich, and L. C. Ho. A 20,000  $M_{\odot}$  Black Hole in the Stellar Cluster G1. *ApJL*, 578:L41–L45, October 2002.
72. K. Gebhardt, R. M. Rich, and L. C. Ho. An Intermediate-Mass Black Hole in the Globular Cluster G1: Improved Significance from New Keck and Hubble Space Telescope Observations. *ApJ*, 634:1093–1102, December 2005.
73. N. Y. Gnedin and J. P. Ostriker. Reionization of the Universe and the Early Production of Metals. *ApJ*, 486:581, September 1997.
74. J. Goodman. Self-gravity and quasi-stellar object discs. *MNRAS*, 339:937–948, March 2003.
75. S. Goswami, S. Umbreit, M. Bierbaum, and F. A. Rasio. Formation of Massive Black Holes in Dense Star Clusters. II. IMF and Primordial Mass Segregation. *ArXiv e-prints*, May 2011.
76. A. Gould and H.-W. Rix. Binary Black Hole Mergers from Planet-like Migrations. *ApJL*, 532:L29–L32, March 2000.
77. T. Greif, V. Springel, S. White, S. Glover, P. Clark, R. Smith, R. Klessen, and V. Bromm. Simulations on a Moving Mesh: The Clustered Formation of Population III Protostars. *ArXiv e-prints*, January 2011.
78. T. Greif, S. White, R. Klessen, and V. Springel. The Delay of Population III Star Formation by Supersonic Streaming Velocities. *ArXiv e-prints*, January 2011.
79. J. Greiner, T. Krühler, J. P. U. Fynbo, A. Rossi, R. Schwarz, S. Klose, S. Savaglio, N. R. Tanvir, S. McBreen, T. Totani, B. B. Zhang, X. F. Wu, D. Watson, S. D. Barthelmy, A. P. Beardmore, P. Ferrero, N. Gehrels, D. A. Kann, N. Kawai, A. K. Yoldaş, P. Mészáros, B. Milvang-Jensen, S. R. Oates, D. Pierini, P. Schady, K. Toma, P. M. Vreeswijk, A. Yoldaş, B. Zhang, P. Afonso, K. Aoki, D. N. Burrows, C. Clemens, R. Filgas, Z. Haiman, D. H. Hartmann, G. Hasinger, J. Hjorth, E. Jehin, A. J. Levan, E. W. Liang, D. Malesani, T.-S. Pyo, S. Schulze, G. Szokoly, K. Terada, and K. Wiersema. GRB 080913 at Redshift 6.7. *ApJ*, 693:1610–1620, March 2009.
80. A. Gualandris and D. Merritt. Ejection of Supermassive Black Holes from Galaxy Cores. *ApJ*, 678:780–797, May 2008.
81. J. Guedes, P. Madau, M. Kuhlen, J. Diemand, and M. Zemp. Simulations of Recoiling Massive Black Holes in the Via Lactea Halo. *ApJ*, 702:890–900, September 2009.
82. J. Guedes, P. Madau, L. Mayer, and S. Callegari. Recoiling Massive Black Holes in Gas-rich Galaxy Mergers. *ApJ*, 729:125, March 2011.
83. M. A. Gürkan, M. Freitag, and F. A. Rasio. Formation of Massive Black Holes in Dense Star Clusters. I. Mass Segregation and Core Collapse. *ApJ*, 604:632–652, April 2004.
84. M. G. Haehnelt, P. Natarajan, and M. J. Rees. High-redshift galaxies, their active nuclei and central black holes. *MNRAS*, 300:817–827, November 1998.
85. M. G. Haehnelt and M. J. Rees. The formation of nuclei in newly formed galaxies and the evolution of the quasar population. *MNRAS*, 263:168–178, July 1993.
86. Z. Haiman. Constraints from Gravitational Recoil on the Growth of Supermassive Black Holes at High Redshift. *ApJ*, 613:36–40, September 2004.
87. Z. Haiman. Galaxy formation: Caught in the act? *Nature*, 430:979–980, August 2004.
88. Z. Haiman, T. Abel, and M. J. Rees. The Radiative Feedback of the First Cosmological Objects. *ApJ*, 534:11–24, May 2000.
89. Z. Haiman and G. L. Bryan. Was Star Formation Suppressed in High-Redshift Minihalos? *ApJ*, 650:7–11, October 2006.
90. Z. Haiman and R. Cen. A Constraint on the Gravitational Lensing Magnification and Age of the Redshift  $z=6.28$  Quasar SDSS 1030+0524. *ApJ*, 578:702–707, October 2002.
91. Z. Haiman, L. Ciotti, and J. P. Ostriker. Reasoning From Fossils: Learning from the Local Black Hole Population about the Evolution of Quasars. *ApJ*, 606:763–773, May 2004.
92. Z. Haiman and G. P. Holder. The Reionization History at High Redshifts. I. Physical Models and New Constraints from Cosmic Microwave Background Polarization. *ApJ*, 595:1–12, September 2003.
93. Z. Haiman and L. Hui. Constraining the Lifetime of Quasars from Their Spatial Clustering. *ApJ*, 547:27–38, January 2001.
94. Z. Haiman, R. Jimenez, and M. Bernardi. Reconstructing the Cosmic Evolution of Quasars from the Age Distribution of Local Early-Type Galaxies. *ApJ*, 658:721–730, April 2007.

95. Z. Haiman, B. Kocsis, and K. Menou. The Population of Viscosity- and Gravitational Wave-driven Supermassive Black Hole Binaries Among Luminous Active Galactic Nuclei. *ApJ*, 700:1952–1969, August 2009.
96. Z. Haiman and A. Loeb. Detection of the First Star Clusters With NGST. In E. P. Smith & A. Koratkar, editor, *Science With The NGST*, volume 133 of *Astronomical Society of the Pacific Conference Series*, page 251, 1998.
97. Z. Haiman and A. Loeb. Observational Signatures of the First Quasars. *ApJ*, 503:505, August 1998.
98. Z. Haiman and A. Loeb. Determining the Redshift of Reionization from the Spectra of High-Redshift Sources. *ApJ*, 519:479–485, July 1999.
99. Z. Haiman and A. Loeb. What Is the Highest Plausible Redshift of Luminous Quasars? *ApJ*, 552:459–463, May 2001.
100. Z. Haiman and E. Quataert. The Formation and Evolution of the First Massive Black Holes. In A. J. Barger, editor, *Supermassive Black Holes in the Distant Universe*, volume 308 of *Astrophysics and Space Science Library*, page 147, August 2004.
101. Z. Haiman, E. Quataert, and G. C. Bower. Modeling the Counts of Faint Radio-Loud Quasars: Constraints on the Supermassive Black Hole Population and Predictions for High Redshift. *ApJ*, 612:698–705, September 2004.
102. Z. Haiman, M. J. Rees, and A. Loeb. Destruction of Molecular Hydrogen during Cosmological Reionization. *ApJ*, 476:458, February 1997.
103. Z. Haiman, A. A. Thoul, and A. Loeb. Cosmological Formation of Low-Mass Objects. *ApJ*, 464:523, June 1996.
104. J. B. Haislip, M. C. Nysewander, D. E. Reichart, A. Levan, N. Tanvir, S. B. Cenko, D. B. Fox, P. A. Price, A. J. Castro-Tirado, J. Gorosabel, C. R. Evans, E. Figueredo, C. L. MacLeod, J. R. Kirschbrow, M. Jelinek, S. Guziy, A. D. U. Postigo, E. S. Cypriano, A. Lacluyze, J. Graham, R. Priddey, R. Chapman, J. Rhoads, A. S. Fruchter, D. Q. Lamb, C. Kouveliotou, R. A. M. J. Wijers, M. B. Bayliss, B. P. Schmidt, A. M. Soderberg, S. R. Kulkarni, F. A. Harrison, D. S. Moon, A. Gal-Yam, M. M. Kasliwal, R. Hudec, S. Vitek, P. Kubanek, J. A. Crain, A. C. Foster, J. C. Clemens, J. W. Bartelme, R. Canterna, D. H. Hartmann, A. A. Henden, S. Klose, H.-S. Park, G. G. Williams, E. Rol, P. O'Brien, D. Bersier, F. Prada, S. Pizarro, D. Maturana, P. Ugarte, A. Alvarez, A. J. M. Fernandez, M. J. Jarvis, M. Moles, E. Alfaro, K. M. Ivarsen, N. D. Kumar, C. E. Mack, C. M. Zdarowicz, N. Gehrels, S. Barthelmy, and D. N. Burrows. A photometric redshift of  $z = 6.39 \pm 0.12$  for GRB 050904. *Nature*, 440:181–183, March 2006.
105. J. F. Hawley and S. A. Balbus. The Dynamical Structure of Nonradiative Black Hole Accretion Flows. *ApJ*, 573:738–748, July 2002.
106. A. Heger, C. L. Fryer, S. E. Woosley, N. Langer, and D. H. Hartmann. How Massive Single Stars End Their Life. *ApJ*, 591:288–300, July 2003.
107. D. C. Heggie. Binary evolution in stellar dynamics. *MNRAS*, 173:729–787, December 1975.
108. T. Hirasawa. Formation of Protogalaxies and Molecular Processes in Hydrogen Gas. *Progress of Theoretical Physics*, 42:523–543, September 1969.
109. L. C. Ho. The CO Tully-Fisher Relation and Implications for the Host Galaxies of High-Redshift Quasars. *ApJ*, 669:821–829, November 2007.
110. L. Hoffman and A. Loeb. Dynamics of triple black hole systems in hierarchically merging massive galaxies. *MNRAS*, 377:957–976, May 2007.
111. F. Hoyle and W. A. Fowler. On the nature of strong radio sources. *MNRAS*, 125:169, 1963.
112. S. A. Hughes and R. D. Blandford. Black Hole Mass and Spin Coevolution by Mergers. *ApJL*, 585:L101–L104, March 2003.
113. P. Hut, S. McMillan, J. Goodman, M. Mateo, E. S. Phinney, C. Pryor, H. B. Richer, F. Verbunt, and M. Weinberg. Binaries in globular clusters. *PASP*, 104:981–1034, November 1992.
114. I. V. Igumenshchev, R. Narayan, and M. A. Abramowicz. Three-dimensional Magnetohydrodynamic Simulations of Radiatively Inefficient Accretion Flows. *ApJ*, 592:1042–1059, August 2003.
115. F. Iocco, A. Bressan, E. Ripamonti, R. Schneider, A. Ferrara, and P. Marigo. Dark matter annihilation effects on the first stars. *MNRAS*, 390:1655–1669, November 2008.

116. R. R. Islam, J. E. Taylor, and J. Silk. Massive black hole remnants of the first stars in galactic haloes. *MNRAS*, 340:647–656, April 2003.
117. R. R. Islam, J. E. Taylor, and J. Silk. Massive black hole remnants of the first stars - III. Observational signatures from the past. *MNRAS*, 354:629–640, October 2004.
118. A. Jenkins, C. S. Frenk, S. D. M. White, J. M. Colberg, S. Cole, A. E. Evrard, H. M. P. Couchman, and N. Yoshida. The mass function of dark matter haloes. *MNRAS*, 321:372–384, February 2001.
119. L. Jiang, X. Fan, F. Bian, J. Annis, K. Chiu, S. Jester, H. Lin, R. H. Lupton, G. T. Richards, M. A. Strauss, V. Malanushenko, E. Malanushenko, and D. P. Schneider. A Survey of  $z \approx 6$  Quasars in the Sloan Digital Sky Survey Deep Stripe. II. Discovery of Six Quasars at  $z_{AB} \gtrsim 21$ . *AJ*, 138:305–311, July 2009.
120. L. Jiang, X. Fan, W. N. Brandt, C. L. Carilli, E. Egami, D. C. Hines, J. D. Kurk, G. T. Richards, Y. Shen, M. A. Strauss, M. Vestergaard, and F. Walter. Dust-free quasars in the early Universe. *Nature*, 464:380–383, March 2010.
121. L. Jiang, X. Fan, M. Vestergaard, J. D. Kurk, F. Walter, B. C. Kelly, and M. A. Strauss. Gemini Near-Infrared Spectroscopy of Luminous  $z \approx 6$  Quasars: Chemical Abundances, Black Hole Masses, and Mg II Absorption. *AJ*, 134:1150, September 2007.
122. R. Jimenez and Z. Haiman. Significant primordial star formation at redshifts  $z \sim 3.4$ . *Nature*, 440:501–504, March 2006.
123. P. Kaaret, H. Feng, and M. Gorski. A Major X-Ray Outburst From an Ultraluminous X-Ray Source in M82. *ApJ*, 692:653–658, February 2009.
124. P. Kaaret, A. H. Prestwich, A. Zezas, S. S. Murray, D.-W. Kim, R. E. Kilgard, E. M. Schlegel, and M. J. Ward. Chandra High-Resolution Camera observations of the luminous X-ray source in the starburst galaxy M82. *MNRAS*, 321:L29–L32, February 2001.
125. H. Kang and P. R. Shapiro. Radiative shocks and hydrogen molecules in pregalactic gas - The effects of postshock radiation. *ApJ*, 386:432–451, February 1992.
126. H. Kang, P. R. Shapiro, S. M. Fall, and M. J. Rees. Radiative shocks inside protogalaxies and the origin of globular clusters. *ApJ*, 363:488–498, November 1990.
127. A. Kashlinsky and M. J. Rees. Formation of population III stars and pregalactic evolution. *MNRAS*, 205:955–971, December 1983.
128. S. Kaspi, P. S. Smith, H. Netzer, D. Maoz, B. T. Jannuzi, and U. Givon. Reverberation Measurements for 17 Quasars and the Size-Mass-Luminosity Relations in Active Galactic Nuclei. *ApJ*, 533:631–649, April 2000.
129. N. Kawai, G. Kosugi, K. Aoki, T. Yamada, T. Totani, K. Ohta, M. Iye, T. Hattori, W. Aoki, H. Furusawa, K. Hurley, K. S. Kawabata, N. Kobayashi, Y. Komiyama, Y. Mizumoto, K. Nomoto, J. Noumaru, R. Ogasawara, R. Sato, K. Sekiguchi, Y. Shirasaki, M. Suzuki, T. Takata, T. Tamagawa, H. Terada, J. Watanabe, Y. Yatsu, and A. Yoshida. An optical spectrum of the afterglow of a  $\gamma$ -ray burst at a redshift of  $z = 6.295$ . *Nature*, 440:184–186, March 2006.
130. C. R. Keeton, M. Kuhlen, and Z. Haiman. Gravitational Lensing Magnification without Multiple Imaging. *ApJ*, 621:559–573, March 2005.
131. D. Kereš, N. Katz, D. H. Weinberg, and R. Davé. How do galaxies get their gas? *MNRAS*, 363:2–28, October 2005.
132. A. R. King, M. B. Davies, M. J. Ward, G. Fabbiano, and M. Elvis. Ultraluminous X-Ray Sources in External Galaxies. *ApJL*, 552:L109–L112, May 2001.
133. T. Kitayama and S. Ikeuchi. Formation of Subgalactic Clouds under Ultraviolet Background Radiation. *ApJ*, 529:615–634, February 2000.
134. C. S. Kochanek. Gravitational Lenses and NGST. In E. P. Smith & A. Koratkar, editor, *Science With The NGST*, volume 133 of *Astronomical Society of the Pacific Conference Series*, page 96, 1998.
135. B. Kocsis and A. Sesana. Gas-driven massive black hole binaries: signatures in the nHz gravitational wave background. *MNRAS*, 411:1467–1479, March 2011.
136. J. A. Kollmeier, C. A. Onken, C. S. Kochanek, A. Gould, D. H. Weinberg, M. Dietrich, R. Cool, A. Dey, D. J. Eisenstein, B. T. Jannuzi, E. Le Floch, and D. Stern. Black Hole Masses and Eddington Ratios at  $0.3 < z < 4$ . *ApJ*, 648:128–139, September 2006.

137. E. Komatsu, K. M. Smith, J. Dunkley, C. L. Bennett, B. Gold, G. Hinshaw, N. Jarosik, D. Larson, M. R.olta, L. Page, D. N. Spergel, M. Halpern, R. S. Hill, A. Kogut, M. Limon, S. S. Meyer, N. Odegard, G. S. Tucker, J. L. Weiland, E. Wollack, and E. L. Wright. Seven-year Wilkinson Microwave Anisotropy Probe (WMAP) Observations: Cosmological Interpretation. *ApJS*, 192:18, February 2011.
138. S. M. Koushiappas, J. S. Bullock, and A. Dekel. Massive black hole seeds from low angular momentum material. *MNRAS*, 354:292–304, October 2004.
139. J. D. Kurk, F. Walter, X. Fan, L. Jiang, S. Jester, H.-W. Rix, and D. A. Riechers. Near-Infrared Spectroscopy of SDSS J0303 - 0019: A Low-luminosity, High-Eddington-Ratio Quasar at  $z \sim 6$ . *ApJ*, 702:833–837, September 2009.
140. J. D. Kurk, F. Walter, X. Fan, L. Jiang, D. A. Riechers, H.-W. Rix, L. Pentericci, M. A. Strauss, C. Carilli, and S. Wagner. Black Hole Masses and Enrichment of  $z \sim 6$  SDSS Quasars. *ApJ*, 669:32–44, November 2007.
141. D. Q. Lamb and D. E. Reichart. Gamma-Ray Bursts as a Probe of the Very High Redshift Universe. *ApJ*, 536:1–18, June 2000.
142. R. N. Lang and S. A. Hughes. Measuring coalescing massive binary black holes with gravitational waves: The impact of spin-induced precession. *Phys. Rev. D*, 74(12):122001, December 2006.
143. M. A. Latif, D. R. G. Schleicher, M. Spaans, and S. Zaroubi. Lyman  $\alpha$  emission from the first galaxies: signatures of accretion and infall in the presence of line trapping. *MNRAS*, 413:L33–L37, May 2011.
144. M. A. Latif, S. Zaroubi, and M. Spaans. The impact of Lyman  $\alpha$  trapping on the formation of primordial objects. *MNRAS*, 411:1659–1670, March 2011.
145. T. R. Lauer, S. M. Faber, D. Richstone, K. Gebhardt, S. Tremaine, M. Postman, A. Dressler, M. C. Aller, A. V. Filippenko, R. Green, L. C. Ho, J. Kormendy, J. Magorrian, and J. Pinkney. The Masses of Nuclear Black Holes in Luminous Elliptical Galaxies and Implications for the Space Density of the Most Massive Black Holes. *ApJ*, 662:808–834, June 2007.
146. A. Lawrence, S. J. Warren, O. Almaini, A. C. Edge, N. C. Hambly, R. F. Jameson, P. Lucas, M. Casali, A. Adamson, S. Dye, J. P. Emerson, S. Foucaud, P. Hewett, P. Hirst, S. T. Hodgkin, M. J. Irwin, N. Lodieu, R. G. McMahon, C. Simpson, I. Smail, D. Mortlock, and M. Folger. The UKIRT Infrared Deep Sky Survey (UKIDSS). *MNRAS*, 379:1599–1617, August 2007.
147. H. M. Lee. Dynamical effects of successive mergers on the evolution of spherical stellar systems. *ApJ*, 319:801–818, August 1987.
148. S. Lepp and J. M. Shull. Molecules in the early universe. *ApJ*, 280:465–469, May 1984.
149. Y. Li, Z. Haiman, and M.-M. Mac Low. Correlations between Central Massive Objects and Their Host Galaxies: From Bulgeless Spirals to Ellipticals. *ApJ*, 663:61–70, July 2007.
150. Y. Li, L. Hernquist, B. Robertson, T. J. Cox, P. F. Hopkins, V. Springel, L. Gao, T. Di Matteo, A. R. Zentner, A. Jenkins, and N. Yoshida. Formation of  $z \sim 6$  Quasars from Hierarchical Galaxy Mergers. *ApJ*, 665:187–208, August 2007.
151. Z. Lippai, Z. Frei, and Z. Haiman. Prompt Shocks in the Gas Disk around a Recoiling Supermassive Black Hole Binary. *ApJL*, 676:L5–L8, March 2008.
152. G. Lodato and P. Natarajan. Supermassive black hole formation during the assembly of pre-galactic discs. *MNRAS*, 371:1813–1823, October 2006.
153. Z. Lukić, K. Heitmann, S. Habib, S. Bashinsky, and P. M. Ricker. The Halo Mass Function: High-Redshift Evolution and Universality. *ApJ*, 671:1160–1181, December 2007.
154. M. E. Machacek, G. L. Bryan, and T. Abel. Simulations of Pregalactic Structure Formation with Radiative Feedback. *ApJ*, 548:509–521, February 2001.
155. P. Madau, A. Ferrara, and M. J. Rees. Early Metal Enrichment of the Intergalactic Medium by Pregalactic Outflows. *ApJ*, 555:92–105, July 2001.
156. P. Madau and E. Quataert. The Effect of Gravitational-Wave Recoil on the Demography of Massive Black Holes. *ApJL*, 606:L17–L20, May 2004.
157. P. Madau and M. J. Rees. Massive Black Holes as Population III Remnants. *ApJL*, 551:L27–L30, April 2001.
158. F. Mahmood Khan, A. Just, and D. Merritt. Efficient Merger of Binary Supermassive Black Holes in Merging Galaxies. *ApJ*, 732:89, May 2011.

159. U. Maio, L. V. E. Koopmans, and B. Ciardi. The impact of primordial supersonic flows on early structure formation, reionization and the lowest-mass dwarf galaxies. *MNRAS*, 412:L40–L44, March 2011.
160. P. Martini. QSO Lifetimes. *Coevolution of Black Holes and Galaxies*, page 169, 2004.
161. P. Martini and D. H. Weinberg. Quasar Clustering and the Lifetime of Quasars. *ApJ*, 547:12–26, January 2001.
162. T. Matsuda, H. Satō, and H. Takeda. Cooling of Pre-Galactic Gas Clouds by Hydrogen Molecule. *Progress of Theoretical Physics*, 42:219–233, August 1969.
163. I. D. McGreer, R. H. Becker, D. J. Helfand, and R. L. White. Discovery of a  $z = 6.1$  Radio-Loud Quasar in the NOAO Deep Wide Field Survey. *ApJ*, 652:157–162, November 2006.
164. I. D. McGreer, P. B. Hall, X. Fan, F. Bian, N. Inada, M. Oguri, M. A. Strauss, D. P. Schneider, and K. Farnsworth. SDSS J094604.90+183541.8: A Gravitationally Lensed Quasar at  $z = 4.8$ . *AJ*, 140:370–378, August 2010.
165. C. F. McKee and J. C. Tan. The Formation of the First Stars. II. Radiative Feedback Processes and Implications for the Initial Mass Function. *ApJ*, 681:771–797, July 2008.
166. S. T. McWilliams, J. I. Thorpe, J. G. Baker, and B. J. Kelly. Impact of mergers on LISA parameter estimation for nonspinning black hole binaries. *Phys. Rev. D*, 81(6):064014, March 2010.
167. K. Menou, Z. Haiman, and V. K. Narayanan. The Merger History of Supermassive Black Holes in Galaxies. *ApJ*, 558:535–542, September 2001.
168. D. Merritt and M. Milosavljević. Massive Black Hole Binary Evolution. *Living Reviews in Relativity*, 8:8, November 2005.
169. D. Merritt and M. Y. Poon. Chaotic Loss Cones and Black Hole Fueling. *ApJ*, 606:788–798, May 2004.
170. A. Mesinger, G. L. Bryan, and Z. Haiman. Ultraviolet Radiative Feedback on High-Redshift Protogalaxies. *ApJ*, 648:835–851, September 2006.
171. A. Mesinger, G. L. Bryan, and Z. Haiman. Relic HII regions and radiative feedback at high redshifts. *MNRAS*, 399:1650–1662, November 2009.
172. M. C. Miller and E. J. M. Colbert. Intermediate-Mass Black Holes. *International Journal of Modern Physics D*, 13:1–64, January 2004.
173. M. Milosavljević, V. Bromm, S. M. Couch, and S. P. Oh. Accretion onto “Seed” Black Holes in the First Galaxies. *ApJ*, 698:766–780, June 2009.
174. M. Milosavljević, S. M. Couch, and V. Bromm. Accretion Onto Intermediate-Mass Black Holes in Dense Protogalactic Clouds. *ApJL*, 696:L146–L149, May 2009.
175. J. Miralda-Escudé and J. A. Kollmeier. Star Captures by Quasar Accretion Disks: A Possible Explanation of the  $M$ - $\sigma$  Relation. *ApJ*, 619:30–40, January 2005.
176. S. Naoz, S. Noter, and R. Barkana. The first stars in the Universe. *MNRAS*, 373:L98–L102, November 2006.
177. J. F. Navarro, C. S. Frenk, and S. D. M. White. A Universal Density Profile from Hierarchical Clustering. *ApJ*, 490:493, December 1997.
178. J. F. Navarro and M. Steinmetz. The Effects of a Photoionizing Ultraviolet Background on the Formation of Disk Galaxies. *ApJ*, 478:13, March 1997.
179. H. Netzer. The Largest Black Holes and the Most Luminous Galaxies. *ApJL*, 583:L5–L8, January 2003.
180. E. Noyola, K. Gebhardt, and M. Bergmann. Gemini and Hubble Space Telescope Evidence for an Intermediate-Mass Black Hole in  $\omega$  Centauri. *ApJ*, 676:1008–1015, April 2008.
181. S. P. Oh. Reionization by Hard Photons. I. X-Rays from the First Star Clusters. *ApJ*, 553:499–512, June 2001.
182. S. P. Oh and Z. Haiman. Second-Generation Objects in the Universe: Radiative Cooling and Collapse of Halos with Virial Temperatures above  $10^4$  K. *ApJ*, 569:558–572, April 2002.
183. S. P. Oh, Z. Haiman, and M. J. Rees. HE II Recombination Lines from the First Luminous Objects. *ApJ*, 553:73–77, May 2001.
184. R. M. O’Leary, F. A. Rasio, J. M. Fregeau, N. Ivanova, and R. O’Shaughnessy. Binary Mergers and Growth of Black Holes in Dense Star Clusters. *ApJ*, 637:937–951, February 2006.



185. K. Omukai. Primordial Star Formation under Far-Ultraviolet Radiation. *ApJ*, 546:635–651, January 2001.
186. K. Omukai, R. Schneider, and Z. Haiman. Can Supermassive Black Holes Form in Metal-enriched High-Redshift Protogalaxies? *ApJ*, 686:801–814, October 2008.
187. B. W. O’Shea and M. L. Norman. Population III Star Formation in a  $\Lambda$ CDM Universe. I. The Effect of Formation Redshift and Environment on Protostellar Accretion Rate. *ApJ*, 654:66–92, January 2007.
188. J. P. Ostriker. Collisional Dark Matter and the Origin of Massive Black Holes. *Physical Review Letters*, 84:5258–5260, June 2000.
189. J. P. Ostriker and N. Y. Gnedin. Reheating of the Universe and Population III. *ApJL*, 472:L63+, December 1996.
190. F. Palla, E. E. Salpeter, and S. W. Stahler. Primordial star formation - The role of molecular hydrogen. *ApJ*, 271:632–641, August 1983.
191. F. I. Pelupessy, T. Di Matteo, and B. Ciardi. How Rapidly Do Supermassive Black Hole “Seeds” Grow at Early Times? *ApJ*, 665:107–119, August 2007.
192. S. F. Portegies Zwart and S. L. W. McMillan. The Runaway Growth of Intermediate-Mass Black Holes in Dense Star Clusters. *ApJ*, 576:899–907, September 2002.
193. W. H. Press and P. Schechter. Formation of Galaxies and Clusters of Galaxies by Self-Similar Gravitational Condensation. *ApJ*, 187:425–438, February 1974.
194. M. Preto, I. Berentzen, P. Berczik, and R. Spurzem. Fast Coalescence of Massive Black Hole Binaries from Mergers of Galactic Nuclei: Implications for Low-frequency Gravitational-wave Astrophysics. *ApJL*, 732:L26+, May 2011.
195. J. Prieto, P. Padoan, R. Jimenez, and L. Infante. Population III Stars from Turbulent Fragmentation at Redshift  $\sim 11$ . *ApJL*, 731:L38+, April 2011.
196. D. Proga and M. C. Begelman. Accretion of Low Angular Momentum Material onto Black Holes: Two-dimensional Magnetohydrodynamic Case. *ApJ*, 592:767–781, August 2003.
197. E. Quataert and A. Gruzinov. Constraining the Accretion Rate onto Sagittarius A\* Using Linear Polarization. *ApJ*, 545:842–846, December 2000.
198. G. D. Quinlan and S. L. Shapiro. The dynamical evolution of dense star clusters in galactic nuclei. *ApJ*, 356:483–500, June 1990.
199. F. A. Rasio, M. Freitag, and M. A. Gürkan. Formation of Massive Black Holes in Dense Star Clusters. *Coevolution of Black Holes and Galaxies*, page 138, 2004.
200. D. S. Reed, R. Bower, C. S. Frenk, A. Jenkins, and T. Theuns. The halo mass function from the dark ages through the present day. *MNRAS*, 374:2–15, January 2007.
201. M. J. Rees. Black Hole Models for Active Galactic Nuclei. *ARA&A*, 22:471–506, 1984.
202. M. J. Rees and J. P. Ostriker. Cooling, dynamics and fragmentation of massive gas clouds - Clues to the masses and radii of galaxies and clusters. *MNRAS*, 179:541–559, June 1977.
203. J. A. Regan and M. G. Haehnelt. The formation of compact massive self-gravitating discs in metal-free haloes with virial temperatures of  $\sim 13000$ – $30000$ K. *MNRAS*, 393:858–871, March 2009.
204. G. T. Richards, M. A. Strauss, B. Pindor, Z. Haiman, X. Fan, D. Eisenstein, D. P. Schneider, N. A. Bahcall, J. Brinkmann, and R. Brunner. A Snapshot Survey for Gravitational Lenses among  $z \gtrsim 4.0$  Quasars. I. The  $z \gtrsim 5.7$  Sample. *AJ*, 127:1305–1312, March 2004.
205. E. Ripamonti, F. Iocco, A. Ferrara, R. Schneider, A. Bressan, and P. Marigo. First star formation with dark matter annihilation. *MNRAS*, page 883, June 2010.
206. M. Saijo, T. W. Baumgarte, S. L. Shapiro, and M. Shibata. Collapse of a Rotating Supermassive Star to a Supermassive Black Hole: Post-Newtonian Simulations. *ApJ*, 569:349–361, April 2002.
207. R. Salvaterra, M. Della Valle, S. Campana, G. Chincarini, S. Covino, P. D’Avanzo, A. Fernández-Soto, C. Guidorzi, F. Mannucci, R. Margutti, C. C. Thöne, L. A. Antonelli, S. D. Barthelmy, M. de Pasquale, V. D’Elia, F. Fiore, D. Fugazza, L. K. Hunt, E. Maiorano, S. Marinoni, F. E. Marshall, E. Molinari, J. Nousek, E. Pian, J. L. Racusin, L. Stella, L. Amati, G. Andreuzzi, G. Cusumano, E. E. Fenimore, P. Ferrero, P. Giommi, D. Guetta, S. T. Holland, K. Hurley, G. L. Israel, J. Mao, C. B. Markwardt, N. Masetti, C. Pagani, E. Palazzi, D. M. Palmer, S. Piranomonte, G. Tagliaferri, and V. Testa. GRB090423 at a redshift of  $z \sim 8.1$ . *Nature*, 461:1258–1260, October 2009.

208. S. Salviander, G. A. Shields, K. Gebhardt, M. Bernardi, and J. B. Hyde. In Search of the Largest Velocity Dispersion Galaxies. *ApJ*, 687:828–834, November 2008.
209. W. C. Saslaw, M. J. Valtonen, and S. J. Aarseth. The Gravitational Slingshot and the Structure of Extragalactic Radio Sources. *ApJ*, 190:253–270, June 1974.
210. D. R. G. Schleicher, M. Spaans, and S. C. O. Glover. Black Hole Formation in Primordial Galaxies: Chemical and Radiative Conditions. *ApJL*, 712:L69–L72, March 2010.
211. D. R. G. Schleicher, M. Spaans, and R. S. Klessen. Probing high-redshift quasars with ALMA. I. Expected observables and potential number of sources. *A&A*, 513:A7+, April 2010.
212. A. Sesana, F. Haardt, P. Madau, and M. Volonteri. Low-Frequency Gravitational Radiation from Coalescing Massive Black Hole Binaries in Hierarchical Cosmologies. *ApJ*, 611:623–632, August 2004.
213. A. Sesana, F. Haardt, P. Madau, and M. Volonteri. The Gravitational Wave Signal from Massive Black Hole Binaries and Its Contribution to the LISA Data Stream. *ApJ*, 623:23–30, April 2005.
214. A. Sesana, M. Volonteri, and F. Haardt. The imprint of massive black hole formation models on the LISA data stream. *MNRAS*, 377:1711–1716, June 2007.
215. S. K. Sethi, Z. Haiman, and K. Pandey. Supermassive Black Hole Formation at High Redshifts Through a Primordial Magnetic Field. *ArXiv e-prints*, May 2010.
216. N. I. Shakura and R. A. Sunyaev. Black holes in binary systems. Observational appearance. *A&A*, 24:337–355, 1973.
217. C. Shang, G. L. Bryan, and Z. Haiman. Supermassive black hole formation by direct collapse: keeping protogalactic gas  $H_2$  free in dark matter haloes with virial temperatures  $T_{\text{vir}} \gtrsim 10^4$  K. *MNRAS*, 402:1249–1262, February 2010.
218. F. Shankar. The demography of supermassive black holes: Growing monsters at the heart of galaxies. *New Astronomy Review*, 53:57–77, April 2009.
219. F. Shankar, M. Bernardi, and Z. Haiman. The Evolution of the  $M_{\text{BH}} - \sigma$  Relation Inferred from the Age Distribution of Local Early-Type Galaxies and Active Galactic Nuclei Evolution. *ApJ*, 694:867–878, April 2009.
220. F. Shankar, M. Croce, J. Miralda-Escudé, P. Fosalba, and D. H. Weinberg. On the Radiative Efficiencies, Eddington Ratios, and Duty Cycles of Luminous High-redshift Quasars. *ApJ*, 718:231–250, July 2010.
221. F. Shankar, D. H. Weinberg, and J. Miralda-Escudé. Self-Consistent Models of the AGN and Black Hole Populations: Duty Cycles, Accretion Rates, and the Mean Radiative Efficiency. *ApJ*, 690:20–41, January 2009.
222. F. Shankar, D. H. Weinberg, and Y. Shen. Constraints on black hole duty cycles and the black hole-halo relation from SDSS quasar clustering. *MNRAS*, 406:1959–1966, August 2010.
223. P. R. Shapiro, M. L. Giroux, and A. Babul. Reionization in a cold dark matter universe: The feedback of galaxy formation on the intergalactic medium. *ApJ*, 427:25–50, May 1994.
224. P. R. Shapiro and H. Kang. Hydrogen molecules and the radiative cooling of pregalactic shocks. *ApJ*, 318:32–65, July 1987.
225. S. L. Shapiro. Formation of Supermassive Black Holes: Simulations in General Relativity. *Coevolution of Black Holes and Galaxies*, page 103, 2004.
226. S. L. Shapiro. Spin, Accretion, and the Cosmological Growth of Supermassive Black Holes. *ApJ*, 620:59–68, February 2005.
227. S. L. Shapiro and S. A. Teukolsky. *Black holes, white dwarfs, and neutron stars: The physics of compact objects*. John Wiley and Sons, 1983.
228. P. A. Shaver, J. V. Wall, K. I. Kellermann, C. A. Jackson, and M. R. S. Hawkins. Decrease in the space density of quasars at high redshift. *Nature*, 384:439–441, December 1996.
229. Y. Shen, M. A. Strauss, M. Oguri, J. F. Hennawi, X. Fan, G. T. Richards, P. B. Hall, J. E. Gunn, D. P. Schneider, A. S. Szalay, A. R. Thakar, D. E. Vanden Berk, S. F. Anderson, N. A. Bahcall, A. J. Connolly, and G. R. Knapp. Clustering of High-Redshift ( $z \geq 2.9$ ) Quasars from the Sloan Digital Sky Survey. *AJ*, 133:2222–2241, May 2007.
230. R. K. Sheth, H. J. Mo, and G. Tormen. Ellipsoidal collapse and an improved model for the number and spatial distribution of dark matter haloes. *MNRAS*, 323:1–12, May 2001.



231. M. Shibata and S. L. Shapiro. Collapse of a Rotating Supermassive Star to a Supermassive Black Hole: Fully Relativistic Simulations. *ApJL*, 572:L39–L43, June 2002.
232. G. A. Shields, K. Gebhardt, S. Salvander, B. J. Wills, B. Xie, M. S. Brotherton, J. Yuan, and M. Dietrich. The Black Hole-Bulge Relationship in Quasars. *ApJ*, 583:124–133, January 2003.
233. I. Shlosman and M. C. Begelman. Evolution of self-gravitating accretion disks in active galactic nuclei. *ApJ*, 341:685–691, June 1989.
234. F. H. Shu. Self-similar collapse of isothermal spheres and star formation. *ApJ*, 214:488–497, June 1977.
235. D. Sijacki, V. Springel, and M. G. Haehnelt. Growing the first bright quasars in cosmological simulations of structure formation. *MNRAS*, 400:100–122, November 2009.
236. J. Silk and M. J. Rees. Quasars and galaxy formation. *A&A*, 331:L1–L4, March 1998.
237. J. Silk and M. Spaans. Molecular Lines as Diagnostics of High-Redshift Objects. *ApJL*, 488:L79+, October 1997.
238. J. D. Silverman, P. J. Green, W. A. Barkhouse, D.-W. Kim, M. Kim, B. J. Wilkes, R. A. Cameron, G. Hasinger, B. T. Jannuzi, M. G. Smith, P. S. Smith, and H. Tananbaum. The Luminosity Function of X-Ray-selected Active Galactic Nuclei: Evolution of Supermassive Black Holes at High Redshift. *ApJ*, 679:118–139, May 2008.
239. T. A. Small and R. D. Blandford. Quasar evolution and the growth of black holes. *MNRAS*, 259:725–737, December 1992.
240. M. Spaans and J. Silk. Pregalactic Black Hole Formation with an Atomic Hydrogen Equation of State. *ApJ*, 652:902–906, December 2006.
241. L. Spitzer, Jr. Equipartition and the Formation of Compact Nuclei in Spherical Stellar Systems. *ApJL*, 158:L139+, December 1969.
242. D. Spolyar, P. Bodenheimer, K. Freese, and P. Gondolo. Dark Stars: A New Look at the First Stars in the Universe. *ApJ*, 705:1031–1042, November 2009.
243. Douglas Spolyar, Katherine Freese, and Paolo Gondolo. Dark matter and the first stars: A new phase of stellar evolution. *Phys. Rev. Lett.*, 100(5):051101, Feb 2008.
244. A. Stacy, V. Bromm, and A. Loeb. Effect of Streaming Motion of Baryons Relative to Dark Matter on the Formation of the First Stars. *ApJL*, 730:L1+, March 2011.
245. A. Stacy, V. Bromm, and A. Loeb. Rotation speed of the first stars. *MNRAS*, 413:543–553, May 2011.
246. A. Stacy, T. H. Greif, and V. Bromm. The first stars: formation of binaries and small multiple systems. *MNRAS*, 403:45–60, March 2010.
247. J. M. Stone and J. E. Pringle. Magnetohydrodynamical non-radiative accretion flows in two dimensions. *MNRAS*, 322:461–472, April 2001.
248. J. M. Stone, J. E. Pringle, and M. C. Begelman. Hydrodynamical non-radiative accretion flows in two dimensions. *MNRAS*, 310:1002–1016, December 1999.
249. J. C. Tan and C. F. McKee. The Formation of the First Stars. I. Mass Infall Rates, Accretion Disk Structure, and Protostellar Evolution. *ApJ*, 603:383–400, March 2004.
250. T. Tanaka and Z. Haiman. The Assembly of Supermassive Black Holes at High Redshifts. *ApJ*, 696:1798–1822, May 2009.
251. N. R. Tanvir, D. B. Fox, A. J. Levan, E. Berger, K. Wiersema, J. P. U. Fynbo, A. Cucchiara, T. Krühler, N. Gehrels, J. S. Bloom, J. Greiner, P. A. Evans, E. Rol, F. Olivares, J. Hjorth, P. Jakobsson, J. Farihi, R. Willingale, R. L. C. Starling, S. B. Cenko, D. Perley, J. R. Maund, J. Duke, R. A. M. J. Wijers, A. J. Adamson, A. Allan, M. N. Bremer, D. N. Burrows, A. J. Castro-Tirado, B. Cavanagh, A. de Ugarte Postigo, M. A. Dopita, T. A. Fatkhullin, A. S. Fruchter, R. J. Foley, J. Gorosabel, J. Kennea, T. Kerr, S. Klose, H. A. Krimm, V. N. Komarova, S. R. Kulkarni, A. S. Moskvitin, C. G. Mundell, T. Naylor, K. Page, B. E. Penprase, M. Perri, P. Podsiadlowski, K. Roth, R. E. Rutledge, T. Sakamoto, P. Schady, B. P. Schmidt, A. M. Soderberg, J. Sollerman, A. W. Stephens, G. Stratta, T. N. Ukwatta, D. Watson, E. Westra, T. Wold, and C. Wolf. A  $\gamma$ -ray burst at a redshift of  $z \approx 8.2$ . *Nature*, 461:1254–1257, October 2009.
252. M. Taoso, G. Bertone, G. Meynet, and S. Ekström. Dark matter annihilations in Population III stars. *Phys. Rev. D*, 78(12):123510, December 2008.

253. M. Tegmark, J. Silk, M. J. Rees, A. Blanchard, T. Abel, and F. Palla. How Small Were the First Cosmological Objects? *ApJ*, 474:1, January 1997.
254. A. A. Thoul and D. H. Weinberg. Hydrodynamic Simulations of Galaxy Formation. II. Photoionization and the Formation of Low-Mass Galaxies. *ApJ*, 465:608, July 1996.
255. D. Tseliakhovich, R. Barkana, and C. Hirata. Suppression and Spatial Variation of Early Galaxies and Mini-halos. *ArXiv e-prints*, December 2010.
256. D. Tseliakhovich and C. Hirata. Relative velocity of dark matter and baryonic fluids and the formation of the first structures. *Phys. Rev. D*, 82(8):083520, October 2010.
257. J. Tumlinson, M. L. Giroux, and J. M. Shull. Probing the First Stars with Hydrogen and Helium Recombination Emission. *ApJL*, 550:L1–L5, March 2001.
258. M. J. Turk, T. Abel, and B. O’Shea. The Formation of Population III Binaries from Cosmological Initial Conditions. *Science*, 325:601–, July 2009.
259. E. L. Turner. Quasars and galaxy formation. I - The  $Z$  greater than 4 objects. *AJ*, 101:5–17, January 1991.
260. N. J. Turner, O. M. Blaes, A. Socrates, M. C. Begelman, and S. W. Davis. The Effects of Photon Bubble Instability in Radiation-dominated Accretion Disks. *ApJ*, 624:267–288, May 2005.
261. H. Umeda, N. Yoshida, K. Nomoto, S. Tsuruta, M. Sasaki, and T. Ohkubo. Early Black Hole formation by accretion of gas and dark matter. *Journal of Cosmology and Astro-Particle Physics*, 8:24, August 2009.
262. R. P. van der Marel. Intermediate-mass Black Holes in the Universe: A Review of Formation Theories and Observational Constraints. *Coevolution of Black Holes and Galaxies*, page 37, 2004.
263. R. P. van der Marel, J. Gerssen, P. Guhathakurta, R. C. Peterson, and K. Gebhardt. Hubble Space Telescope Evidence for an Intermediate-Mass Black Hole in the Globular Cluster M15. I. STIS Spectroscopy and WFPC2 Photometry. *AJ*, 124:3255–3269, December 2002.
264. D. E. Vanden Berk, G. T. Richards, A. Bauer, M. A. Strauss, D. P. Schneider, T. M. Heckman, D. G. York, P. B. Hall, X. Fan, G. R. Knapp, S. F. Anderson, J. Annis, N. A. Bahcall, M. Bernardi, J. W. Briggs, J. Brinkmann, R. Brunner, S. Burles, L. Carey, F. J. Castander, A. J. Connolly, J. H. Crocker, I. Csabai, M. Doi, D. Finkbeiner, S. Friedman, J. A. Frieman, M. Fukugita, J. E. Gunn, G. S. Hennessy, Ž. Ivezić, S. Kent, P. Z. Kunszt, D. Q. Lamb, R. F. Leger, D. C. Long, J. Loveday, R. H. Lupton, A. Meiksin, A. Merelli, J. A. Munn, H. J. Newberg, M. Newcomb, R. C. Nichol, R. Owen, J. R. Pier, A. Pope, C. M. Rockosi, D. J. Schlegel, W. A. Siegmund, S. Smee, Y. Snir, C. Stoughton, C. Stubbs, M. SubbaRao, A. S. Szalay, G. P. Szokoly, C. Tremonti, A. Uomoto, P. Waddell, B. Yanny, and W. Zheng. Composite Quasar Spectra from the Sloan Digital Sky Survey. *AJ*, 122:549–564, August 2001.
265. A. Vecchio. LISA observations of rapidly spinning massive black hole binary systems. *Phys. Rev. D*, 70(4):042001, August 2004.
266. M. Vestergaard. Determining Central Black Hole Masses in Distant Active Galaxies. *ApJ*, 571:733–752, June 2002.
267. M. Vestergaard. Early Growth and Efficient Accretion of Massive Black Holes at High Redshift. *ApJ*, 601:676–691, February 2004.
268. M. Vestergaard, X. Fan, C. A. Tremonti, P. S. Osmer, and G. T. Richards. Mass Functions of the Active Black Holes in Distant Quasars from the Sloan Digital Sky Survey Data Release 3. *ApJL*, 674:L1–L4, February 2008.
269. M. Vestergaard and P. S. Osmer. Mass Functions of the Active Black Holes in Distant Quasars from the Large Bright Quasar Survey, the Bright Quasar Survey, and the Color-selected Sample of the SDSS Fall Equatorial Stripe. *ApJ*, 699:800–816, July 2009.
270. E. T. Vishniac. A necessary condition for equilibrium in stellar systems with a continuous mass spectrum. *ApJ*, 223:986–990, August 1978.
271. M. Volonteri. Formation of supermassive black holes. *Astron. Astrophys. Rev.*, 18:279–315, July 2010.
272. M. Volonteri, F. Haardt, and P. Madau. The Assembly and Merging History of Supermassive Black Holes in Hierarchical Models of Galaxy Formation. *ApJ*, 582:559–573, January 2003.

273. M. Volonteri, G. Lodato, and P. Natarajan. The evolution of massive black hole seeds. *MNRAS*, 383:1079–1088, January 2008.
274. M. Volonteri and P. Natarajan. Journey to the  $M_{\text{BH}} - \sigma$  relation: the fate of low-mass black holes in the Universe. *MNRAS*, 400:1911–1918, December 2009.
275. M. Volonteri and M. J. Rees. Rapid Growth of High-Redshift Black Holes. *ApJ*, 633:624–629, November 2005.
276. M. Volonteri and M. J. Rees. Quasars at  $z=6$ : The Survival of the Fittest. *ApJ*, 650:669–678, October 2006.
277. R. V. Wagoner. Physics of Massive Objects. *ARA&A*, 7:553, 1969.
278. F. Walter, F. Bertoldi, C. Carilli, P. Cox, K. Y. Lo, R. Neri, X. Fan, A. Omont, M. A. Strauss, and K. M. Menten. Molecular gas in the host galaxy of a quasar at redshift  $z = 6.42$ . *Nature*, 424:406–408, July 2003.
279. R. Wang, C. L. Carilli, R. Neri, D. A. Riechers, J. Wagg, F. Walter, F. Bertoldi, K. M. Menten, A. Omont, P. Cox, and X. Fan. Molecular Gas in  $z \approx 6$  Quasar Host Galaxies. *ApJ*, 714:699–712, May 2010.
280. R. Wang, J. Wagg, C. L. Carilli, F. Walter, D. A. Riechers, C. Willott, F. Bertoldi, A. Omont, A. Beelen, P. Cox, M. A. Strauss, J. Bergeron, T. Forveille, K. M. Menten, and X. Fan. CO (2-1) Line Emission in Redshift 6 Quasar Host Galaxies. *ArXiv e-prints*, May 2011.
281. G. J. Wasserburg and Y.-Z. Qian. A Model of Metallicity Evolution in the Early Universe. *ApJL*, 538:L99–L102, August 2000.
282. S. D. M. White and M. J. Rees. Core condensation in heavy halos - A two-stage theory for galaxy formation and clustering. *MNRAS*, 183:341–358, May 1978.
283. C. J. Willott, L. Albert, D. Arzoumanian, J. Bergeron, D. Crampton, P. Delorme, J. B. Hutchings, A. Omont, C. Reyl e, and D. Schade. Eddington-limited Accretion and the Black Hole Mass Function at Redshift 6. *AJ*, 140:546–560, August 2010.
284. C. J. Willott, P. Delorme, C. Reyl e, L. Albert, J. Bergeron, D. Crampton, X. Delfosse, T. Forveille, J. B. Hutchings, R. J. McLure, A. Omont, and D. Schade. The Canada-France High- $z$  Quasar Survey: Nine New Quasars and the Luminosity Function at Redshift 6. *AJ*, 139:906–918, March 2010.
285. C. J. Willott, R. J. McLure, and M. J. Jarvis. A  $3 \times 10^9 M_{\odot}$  Black Hole in the Quasar SDSS J1148+5251 at  $z=6.41$ . *ApJL*, 587:L15–L18, April 2003.
286. C. J. Willott, W. J. Percival, R. J. McLure, D. Crampton, J. B. Hutchings, M. J. Jarvis, M. Sawicki, and L. Simard. Imaging of SDSS  $z > 6$  Quasar Fields: Gravitational Lensing, Companion Galaxies, and the Host Dark Matter Halos. *ApJ*, 626:657–665, June 2005.
287. J. H. Wise and T. Abel. Resolving the Formation of Protogalaxies. III. Feedback from the First Stars. *ApJ*, 685:40–56, September 2008.
288. J. H. Wise, M. J. Turk, and T. Abel. Resolving the Formation of Protogalaxies. II. Central Gravitational Collapse. *ApJ*, 682:745–757, August 2008.
289. J. Wolcott-Green, G. L. Bryan, and Z. Haiman. Photodissociation of  $\text{H}_2$  in Protogalaxies: Self-shielding in 3D Simulations. *MNRAS*, *submitted*, *arxiv preprint 1106.xxxx*, June 2011.
290. S. E. Woosley. Gamma-ray bursts from stellar mass accretion disks around black holes. *ApJ*, 405:273–277, March 1993.
291. J. S. B. Wyithe. The shallow slope of the  $z \sim 6$  quasar luminosity function: limits from the lack of multiple-image gravitational lenses. *MNRAS*, 351:1266–1276, July 2004.
292. J. S. B. Wyithe and A. Loeb. Gravitational Lensing of the Sloan Digital Sky Survey High-Redshift Quasars. *ApJ*, 577:57–68, September 2002.
293. J. S. B. Wyithe and A. Loeb. Magnification of light from many distant quasars by gravitational lenses. *Nature*, 417:923–925, June 2002.
294. J. S. B. Wyithe and A. Loeb. Low-Frequency Gravitational Waves from Massive Black Hole Binaries: Predictions for LISA and Pulsar Timing Arrays. *ApJ*, 590:691–706, June 2003.
295. J. S. B. Wyithe and A. Loeb. Self-regulated Growth of Supermassive Black Holes in Galaxies as the Origin of the Optical and X-Ray Luminosity Functions of Quasars. *ApJ*, 595:614–623, October 2003.
296. J. Yoo and J. Miralda-Escud e. Formation of the Black Holes in the Highest Redshift Quasars. *ApJL*, 614:L25–L28, October 2004.

297. S.-C. Yoon, F. Iocco, and S. Akiyama. Evolution of the First Stars with Dark Matter Burning. *ApJL*, 688:L1–L4, November 2008.
298. N. Yoshida, T. Abel, L. Hernquist, and N. Sugiyama. Simulations of Early Structure Formation: Primordial Gas Clouds. *ApJ*, 592:645–663, August 2003.
299. N. Yoshida, K. Omukai, and L. Hernquist. Protostar Formation in the Early Universe. *Science*, 321:669–, August 2008.
300. N. Yoshida, A. Sokasian, L. Hernquist, and V. Springel. Early Structure Formation and Reionization in a Warm Dark Matter Cosmology. *ApJL*, 591:L1–L4, July 2003.
301. Q. Yu. Evolution of massive binary black holes. *MNRAS*, 331:935–958, April 2002.
302. Q. Yu and S. Tremaine. Observational constraints on growth of massive black holes. *MNRAS*, 335:965–976, October 2002.
303. N. Yunes, B. Kocsis, A. Loeb, and Z. Haiman. Imprint of Accretion Disk-Induced Migration on Gravitational Waves from Extreme Mass Ratio Inspirals. *ArXiv e-prints*, March 2011.
304. G. R. Zeimann, R. L. White, R. H. Becker, J. A. Hodge, S. A. Stanford, and G. T. Richards. Discovery of a Radio-Selected  $z \sim 6$  Quasar. *ArXiv e-prints*, May 2011.
305. J. Zhang, O. Fakhouri, and C.-P. Ma. How to grow a healthy merger tree. *MNRAS*, 389:1521–1538, October 2008.
306. H. Zhao, M. G. Haehnelt, and M. J. Rees. Feeding black holes at galactic centres by capture from isothermal cusps. *New Astronomy*, 7:385–394, October 2002.